Particle and trace gas measurements of Eyjafjallajökull 2010

Evolution and ageing of the volcanic ash cloud within Switzerland

Master's Thesis

Faculty of Science

University of Bern

presented by

Sandra Meisser

2011

Supervisor:

Prof. Dr. Stefan Brönnimann
Institute of Geography and Oeschger Centre for Climate Change Research

Co-Supervisor:

Dr. Bruno Neininger
Metair and ZHAW Winterthur

Advisor:

Dr. Ralph Rickli
Institute of Geography and Oeschger Centre for Climate Change Research

"It was something that has never happened before in aviation history. People started traveling like they did 50 years ago - passengers were stranded in Istanbul, and they had to take trains back to Germany from there. Suddenly you realize it takes three days to get somewhere if you can't fly there."

(Stephan Orth, travel editor)

Summary

The volcanic eruptions of Eyjafjallajökull in spring 2010 caused major air traffic disruptions within Europe. The economic and social impact of flight cancellations led to an elusive media interest. Scientists profited from this unique situation by a large number of *in-situ* measurements for further improvements of forecast distribution models and a better understanding of transport and atmospheric chemistry. In this master thesis, the (1) meteorological influences on the volcanic plume characteristics are examined, as well as (2) ageing and (3) chemical processes of the gas and aerosol phase. *In-situ* measurements of Metair and of the Swiss Air Quality Monitoring Network (NABEL) were used for the analysis, as well as distribution and trajectory models. The main findings regarding (1) meteorology are the influence of precipitation (primarily decrease in particulate matter by wash out processes) and wind (strong winds (Föhn) can inject unprocessed VA layers into PBL). (2) Concentrations of both gas and aerosol phase dilute with an identical decrease rate. The gas/aerosol ratio however depends strongly on the weather conditions (low ratio for fair weather) due to different depletion processes. The (3) chemical processes regarding ozone destruction are not completely clear, but are most likely affected by surface reactions with particles and a moderately increased SO_2 concentration in May enhancing the depletion of O_3.

Content

Abbreviations

AMSL	above mean sea level
Ar	argon
BAZL	Federal Office of Civil Aviation
Cl	chlorine
CAPE	convective available potential energy
CO	carbon monoxide
CO_2	carbon dioxide
CPC	condensation particle counter
EMPA	Swiss Federal Laboratories for Material Science and Technology
F	fluorine
FL	flight level; standard nominal altitude for aircraft in hundreds of feet
BAFU	Federal Office for the Environment
GHG	greenhouse gases
H	hydrogen
H_2O	hydrogen oxide / water
HCl	hydrogen chloride
HF	hydrogen fluoride
H_2S	hydrogen sulfate
H_2SO_4	sulfuric acid
IRGA	infrared gas analyser
kts	knots (wind speed)
N	nitrogen
nm	1000nm = 1µm = 10^{-3} mm
OPC	optical particle counter
PBL	planetary boundary layer
PM1, PM10	particles of 1 or 10 micrometers and less (aerodynamic diameter)
ppm, ppb, ppt	parts per million, parts per billion, parts per trillion
PSL	polystyrene latex sphere (used for calibrations)
S	sulfur
SMPS	scanning mobility particle sizer
SO_2	sulfur dioxide
LT	local time
UTC	universal time coordinated
VA	volcanic ash
VAAC	Volcanic Ash Advisory Center
% w/w	weight percentage

1 Introduction

The explosive eruptions of Eyjafjallajökull, Iceland in spring 2010 kept large parts of Europe in suspense. Volcanic particles ascended to the upper levels of the troposphere as well as seldom into the lower stratosphere, and were carried thousands of kilometers towards lower latitudes. The effects of the volcanic eruptions during April and May were characterized by mainly two remarkable consequences. The volcanic ash (VA) plumes caused the largest disruption of air traffic since World War II. Around 100'000 flights were cancelled due to the risk of engine damage caused by particles of the VA plume [Wall and Flottau, 2010; Prata and Tupper, 2009]. The VA plumes implicated complete airspace closures in many countries for several days. Within Switzerland, the Federal Office of Civil Aviation (BAZL) declared a restraint for aircrafts from 16 April until 20 April due to the hazard generated by volcanic ash. Subsequently, a second VA cloud appeared between 8 and 9 May which, unlike the first VA event, did lead to an airspace closure in Southern Germany, Northern Italy and Spain, but not within Switzerland [Bukowiecki et al., 2010]. Besides the major air traffic disruptions in Europe, also Iceland was largely affected by the eruptions. Hundreds of people had to leave their homes as the melting glacier around Eyjafjallajökull led to flash floods destroying infrastructure. Fortunately, no fatalities were reported [Blunden et al., 2011].

Preliminary to the Eyjafjallajökull event in 2010, European air traffic has never been affected in this dimension by any volcanic eruption. Thus, this massive interruption caused large financial consequences thereby increasing the need of knowledge in terms of transport and ageing processes to estimate the VA distribution pattern more reasonable. For the first time, European scientists were enabled to gather data also with airborne *in-situ* measurement systems supplementary to ground- and satellite-based devices due to the close position to the volcano and its plumes. This additional information allows detailed atmospheric cross sections and therefore provides important material for research of atmospheric processes.

The first launched research aircraft in Switzerland was Dimona of Metair [EUFAR, 2010]. Performing several flights during the VA plume days, Metair collected various data of the plume including trace gas measurements and particle size distribution. Beyond other ground-based measurements, these data provided a basis to analyse physical and chemical processes of the VA plume within Switzerland for this master thesis. Mainly three issues were covered by examining the interaction of both phases with meteorology, comparing the concentration dilution rate of both particle and gas phase as well as chemical reactions leading to ozone depletion inside a volcanic ash layer.

- **Interaction with meteorology**

  Characteristics of the particle and gas phase depend on precipitatio, winds and atmospheric stratification. Rain and a high relative humidity is expected to increase the scavenging processes and wash out of aerosols. In weak wind conditions, less particles of the large fraction reach Switzerland as they have more time for gravitational settling between Iceland and Switzerland. Stable atmospheric stratification lead to increased concentration values within PBL because of reduced mixing processes with the FT.

- **Ageing processes**

  Both phases within the VA plume are exposed to the same meteorological conditions. Thus, the dilution rate of the aerosol phase corresponds to the decrease of the gas phase concentration in the same time span. In rainy conditions, it is expected that the particles are washed out faster, whereas the gas phase phase remains nearly constant.

- **Chemical processes**

  Previous large volcanic eruptions showed a decrease in O_3 mostly due to reactive processes with SO_2. Emitted SO_2 of Eyjafjalla is therefore expected to lead to a depletion in O_3 in the respective volcanic air layer.

1.1 Background and motivation

Volcanic eruptions play a relevant part within the earth's atmosphere. Volcanoes emit huge amounts of particles and gases, whose effects could be observed well during the large eruptive events in the past. Sulfur gases reaching the stratosphere are mainly responsible for long-term climatic effects. On the one hand, they lead to an increase in temperature in the respective atmospheric layer due to the absorption of the solar near-infrared radiation. On the other hand, the higher amount of particles increases the short-wave backscattering (figure 1) and therefore reduces temperature on the ground. In general, the second effect exceeds the first process

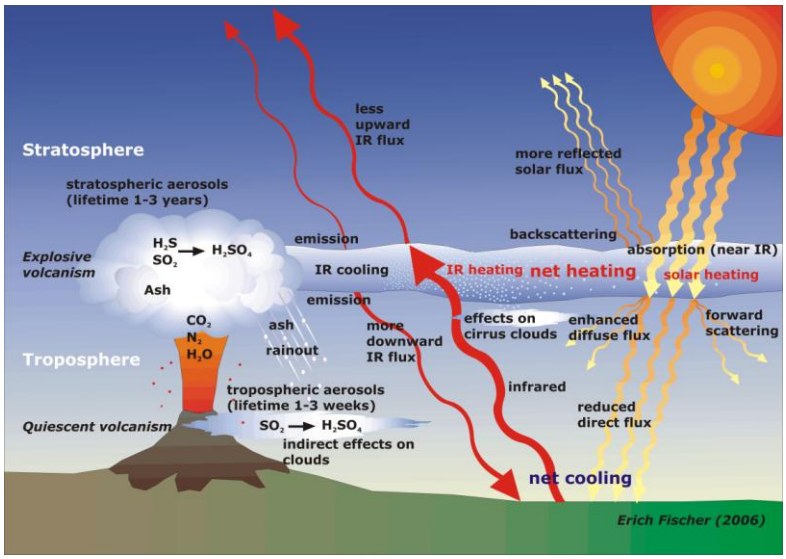

Figure 1: Volcanic processes in troposphere and stratosphere downwind from the vent. (source: Fischer et al., 2006).

and thus leads to global cooling over one or two years [Andersen et al., 2001]. Though, not all the processes are yet well understood and the specific warming and cooling effects of aerosols requires further research [Isaksen et al., 2009]. In the case of Eyjafjallajökull, the climate effect was not measurable, since only a marginal part of the particles and trace gases reached the stratosphere [Blunden et al., 2011; Petersen, 2010. Also the high latitude position of the volcano determines the maximum climatic influence being much lower than that of tropic volcanoes. The volume of the eruptive material and the height of the plume were relatively modest compared to the large plumes of Pinatubo (Phillippines, 1991) and Tambora (Indonesia, 1815). Those tropical eruptions usually have the largest climatic effects, as they are more likely to spread the VA plume across both hemispheres [Brönnimann, 2010].

Hence, a short-period approach examining processes such as the ageing and transport of the volcanic cloud is more appropriate. Due to the quantity of *in-situ* measurements, a higher resolved analysis of atmospheric processes was enabled compared to previous, worse documented volcanic eruptions. Ageing mechanisms, partly caused by rainout, tropopsheric chemical reactions and effects on clouds are only a small number of processes observable in the lower atmosphere (figure 1). The anomalous situation caused by the eruptions in 2010 motivated me to combine the available data of the volcanic ash layers and its related processes with meteorological knowledge gained in the precedent internship with Meteotest.

1.2 Characteristics

The Eyjafjallajökull volcano is a stratovolcano located on the southern coast of Iceland (63.63°N, 19.621° W) with an altitude of 1666 meter above mean sea level (AMSL). The eruption history reaches 800’000 years back in time, but the volcano was active only twice during the past 1’100 years, whereas the flanking Katla volcano erupted 20 times during this time span. The seismic activity of Eyjafjallajökull had been very low for several decades until the 1990s. In 1994 and 1999, the buildup

Figure 2: Phreatomagmatic eruption of Eyjafjallajökull on April 16, 2010 Colliding ash particles lead to a separation of electric charge. This difference induces the formation of lightnings.
(URL: http://www.selectworld.travel/destination-essentials, access: 27.9.2011)

of two intrusions caused an increased seismic activity at Eyjafjallajökull [Sturkell et al., 2010], which were followed by the first eruptions since almost 200 years [Smithonian Institution, 2010]. Iceland is located at the northern end of the diverting mid-atlantic ridge, thus its magma chamber basically contains oceanic magma material with a trachyandesyte-like compo-sition. Trachyandesytes are igneous rocks and composed of preliminary mafic to intermediate minerals containing up to 55-60% w/w SiO_2 in the April and May phase. This rather alkaline to intermediate composition induces usually less explosive eruptions than volcanoes with felsic compositions including higher SiO_2 contents [Smithonian Institution, 2010]. Also, internally dissolved water and other volcanic gases undergo an enormous increase in volume when magma rises to the surface and causes a massive expansion. Besides the magma composition, also the type of eruption is essential regarding the explosivity of a volcano. In the case of glacier-covered Icelandic volcanoes, external water is an important factor and triggers phreatomagmatic eruptions [Gudmundsson, 2005]. The heat of the magma chamber causes the covering glacier to melt (figure 2). The most common theory is that external water acts as a coolant when interacting with hot lava [White, 1996]. The resulting explosive thermal contraction blasts the lava into a vast quantity of particles. Both processes - the interaction with external water as well as the above mentioned magma composition - are the main driving forces for explosive eruptions.

1.3 Eruptive Phase in April and May 2010

Upcoming eruptions have been indicated in March by a continuous increase of seismic activity (table 1), followed by minor fissure eruptions observed in an area named Fimmvörðuháls between the Eyjafjallajökull and Mýrdalsjökull icecaps during late March 2010. Large phreatomagmatic eruptions in mid-April (figure 2) caused the spreading of VA plumes across Europe. After 21 April, eruptions only happened occasionally and the vent mainly produced lava streams [Smithonian Institution, 2010].

Table 1: Duration of phases, specific activities and impacts of Eyjafjallajökull eruptions in 2010.

phase	activity	impacts
4 March – 20 March	continuous increase of seismic activity	seismic signal sources rose slowly towards surface
21 March – 13 April	fissure eruptions ENE of Eyjafjallajökull	lava melts adjacent winter snow resulting in local steam plumes
14 April – 20 April	explosive phreatomagmatic eruptions	VA plumes ascend to upper troposphere spreading across Europe
21 April – End of May	mainly lava production with occasional explosive eruptions	smaller and lower VA plumes with reduced impact on Europe

Considering only the phases of the plume, airborne material can be separated into three phases according to satellite-based trace gas measurements of sulfur dioxide (SO_2). An ash-rich phase in the initial state (mid-April) is followed by a second phase with a lower intensity. Finally, larger amounts of both sulfur dioxide and ash were observed in May [Thomas et al., 2011].

1.4 Objectives

In this master thesis, the core themes are gas and aerosol phases interacting with meteorological patterns; ageing procedures within the volcanic ash layer and chemial processes of certain emission products. Thus, the master thesis is structured as follows: a chapter describing volcanic gas and particle phases and its properties is followed by a section on how these emission products are quantified with *in-situ* measurements of Metair and NABEL. Also Langrangian models simulating the transport of the volcanic ash (VA) plume and its dispersion are taken into account. Meteorological situations and measurement results are presented for both phases in April and May 2010, followed by the discussion of the theses within the same chapter. A conclusion with the most valuable findings and an outlook will complete this piece of work.

2 Aerosols and gas phase

Volcanic emissions consist of various components including primarily water vapor and other gases as well as a phase of particles determined by the geological character of the volcano. Both trace gases and aerosols reveal different characteristics regarding diffusion and chemical reactions. Aerosols are particles and/or liquid droplets and the gas together (figure 3) whereas particles by definition consits of suspended particulate matter.

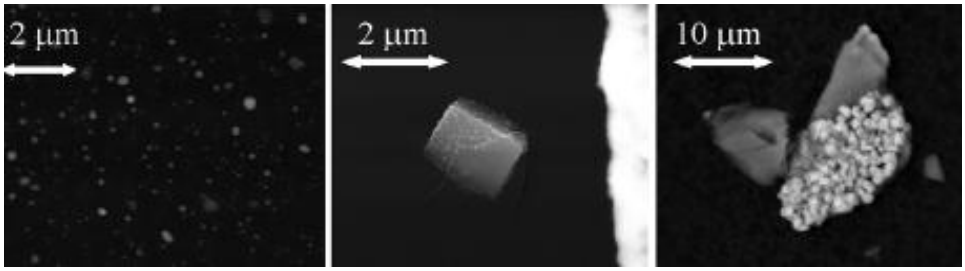

Figure 3: Examples of ammonium sulfate aerosols (left), a silicate aerosol with droplets of ammonium sulfate (middle) and an agglomerate of large silicate particles with iron oxide (right) from a DLR Falcon sample of 2 May 2011 (source: Schumann et al., 2010).

For this work, the following definitions are applied:

- Particles - also known as particulate matter (PM), fine particles or soot – are tiny subdivisions of solid matter suspended in a gas or liquid
- Aerosols refer to particles and/or liquid droplets and the gas together
- The gas phase contains only gaseous molecules

In the context of this work, a *volcanic ash plume* contains not only particles but also liquid aerosols and the gas phase

2.1 Volcanic aerosols

Solid material from volcanoes can be divided into three sections: blocks and bombs (>64mm), lapilli (2-64mm) and ash (<2mm). Ashes are very fine-grained fragments, mostly broken glass shards

(amorphous) and pulverized rocks (crystalline). The fragmentation occurs when water encounters hot magma inside the vent. In a second step their size is reduced again through the eruption of the magma where the sudden cooling causes the particles to abruptly solidify into glass or rock [Degruyter, 2006]. Especially the accumulated and coarse modes are enhanced in VA plumes (see appendix A). The transport of ash is controlled by the windspeed and direction as well as the eruption style. The eruption style/explositivy on the other side defines volume/size of the ash (depending on the rate of magma supply) and the altitude to which the ash rises. The heavier the particles, the earlier they fall out. Also the wash out by precipitation causes a faster settlement of volcanic particles (figure 1). In the case of Eyjafjallajökull, glass shards and most minerals consisted mainly of Si, Al, Mg, Fe and Ca [Bukowiecki et al., 2010]. Small aerosols below 500nm were dominated mainly by ammonium sulfates/nitrates. Larger aerosols consisted primarily of silicates and mixed particles which showed increased concentrations of Cl and S on their surface. This indicates a deposition of volcanic gases on aerosols [Schumann et al., 2010]. Generally, the characteristics of aerosols can be defined by number or mass concentrations; particle size distributions or chemical composition.

2.2 Volcanic gases

Alternatively to free oxygen produced by photosynthesis, all other atmospheric gases originate from inside the earth and can be released by volcanic eruptions. In general, the gaseous phase accounts approximately for 1% to 5% of the total magma weight, whereof water vapor constitutes 70-90%. The remaining amount besides water vapor includes CO_2, SO_2 and trace quantities of N, H, CO, S, Ar, Cl, and F. These supplementary gases may react with hydrogen and water producing toxic compounds such as HCl, HF, H_2SO_4 and H_2S (table 2) [Degruyter, 2006].

Table 2: Some main gases (SO_2 and CO_2) and also the trace gases CO and NO_x are examined within this master thesis.

	Volcanic volatile compounds
main gases	H_2O, CO_2, SO_2
trace gases	N, H, S,F, Ar, CO, Cl
toxic gases	HCl, HF, H_2SO_4, H_2S

The following listing includes those gases which have been analysed by Metair or NABEL during the eruption. Mainly the main gases SO_2 and CO_2, the trace gases CO and NO_x and additionally O_3 as a reaction product.

Sulfuric compounds

The main anthropogenic sources of sulfur in the atmosphere are coal and oil combustion, oil refining and melting of ores, whereas the main natural sources consists of oceanic phytoplankton and volcanoes [Chin et al., 1996]. Emitted sulfur forms SO_2 which can cause acid rain. Smaller active volcanoes emit SO_2 rates of less than 20 tons per day. Larger eruption types like Mount Pinatubo on 15 June 1991 produced up to 500'000 times more (which corresponds to a magma volume of 3-5km^3). This enormous quantity of SO_2 injected into the stratosphere converted into H_2SO_4 and resulted in an approximately 0.6°C cooling of the Earth's surface in the Northern Hemisphere [USGS, 2011]. H_2SO_4 are most effective regarding the backscattering of incoming shortwave radiation and thereby lowering the global temperatures. Even the emitted greenhouse gases (GHG) are commonly not able to compensate this effect. It is estimated that Eyjafjallajökull emitted only around 3'000 tons SO_2 per day, remaining principally within the troposphere where the residence time is clearly lower than in the stratosphere. The atmospheric reactions of SO_2 are very complex, and proceed through three different ways to the sulfate ion (SO_4^{2-}). SO_2 can react with the hydroxyl radical to forming HSO_3 radicals (1) finally converting with another hydroxyl radical (2) into H_2SO_4. Sulfur dioxide also dissolves in water droplets (3) where it reacts with oxygen to SO_4^{2-}. The third pathway (4) to form sulfuric acid is the reaction of sulfur dioxide with hydrogen peroxide.

$$\cdot HO + SO_2 \rightarrow \cdot HOSO_2 \quad (1)$$

$$\cdot HOSO_2 + \cdot HO \rightarrow H_2SO_4 \quad (2)$$

$$SO_2(aq) + O(aq) \rightarrow H_2SO_4 \quad (3)$$

$$SO_2 + \cdot HOSO_2 \rightarrow H_2SO_4 \quad (4)$$

SO_2 is also important to distinguish Saharan dust from volcanic ash. Whereas volanic events emit both PM10 and SO_2, Saharan dust events imply only enhanced PM10 [Flentje et al., 2010]. The particles are in the same concentration dimensions, but differ in terms of the light scattering coefficient σ_{sp} and the light absorbtion coefficient σ_{ap}. The wavelength dependence of the single scattering albedo (SSA= $\sigma_{sp}/(\sigma_{sp} + \sigma_{ap})$) is inversed during Saharan dust events, such that the SSA Ångström exponent becomes negative in the presence of mineral dust [Coen et al., 2004]. During the eruption of Eyjafjallajökull, the Ångström exponent remained positive during April and May indicating that Saharan dust events did not take place.

Carbon dioxide

By far the largest part of CO_2 originates from anthropogenic fossil fuel combustion. Natural sources such as plant and animal respiration, ocean-atmosphere exchange and volcanic emission accounts for only approximately a twentieth of the total emission. Volcanoes release up to 250 million tons of CO_2 into the atmosphere per year. Climatically seen, CO_2 contributes 9-26 % to the greenhouse effect and is therefore the most important anthropogenic and natural GHG. However, the volcanically emitted quantity is still less than 1% of the anthropogenic emitted CO_2. It does not pose a direct

hazard to life because it dilutes very quickly to low concentrations [USGS, 2011]. Additionally, emitted aerosols backscatter solar radiation and therefore mostly overcompensate for the effect of emitted GHG.

Carbon monoxide

CO is largely associated with incomplete combustion. Either anthropogenic (heating, traffic) or natural sources (volcanoes, forest fires) are potential emitters. Volcanic eruptions transmit only a small quantity into the atmosphere where CO remains inert as a meta-stable gas. Inside the planetary boundary layer (PBL), CO is an important trace gas besides CO_2, NO and NO_x [Flentje et al., 2010] and might influence measurements of the VA plume when down-mixing occurs.

Nitrogen oxides

Nitrogen oxides (NO_x= NO and NO_2) are highly reactive and mainly produced by biological processes in soil and atmospheric oxidation of ammonia in the nature. The man-made sources though are of a higher importance. Mostly high-temperature fuel combustions of motor vehicles are responsible for enhanced concentrations of NO in the planetary boundary layer. In the vicinity of large emissions of NO, O_3 concentrations are depressed through the net conversion of O_3 into NO_2. This process takes mainly place within the PBL. In the free troposphere (FT) however, emitted nitrogen oxidizes to NO_2 (5) and can also form nitric acid (6).

$$2NO + O_2 \rightarrow 2NO2 \quad (5)$$

$$4NO_2 + O_2 \rightarrow 4HNO_3 \quad (6)$$

Ozone

O_3 constitutes an exception in relation to trace gases. Although O_3 does not belong to any VA plume component, it indicates atmospheric VA plumes by a decrease in O_3 and is therefore an indirect measurement method. O_3 can be reduced when sulfate aerosols of high rising eruptions reach the stratosphere (similar reaction as in cold stratospheric clouds). Sulfate aerosols promote complex chemical reactions on their surfaces that alter chlorine and nitrogen chemical species in the stratosphere. This effect generates chlorine monoxide, which destroys O_3 [USGS, 2011]. Very low ozone levels, as it happened during the eruption of Mt. Pinatubo, can be the consequence [USGS, 2011]. Also halogenides (Br, Cl) [Gerlach, 2004] contribute to a depletion (basic reactions (7) and (8)).

$$2Br + O_3 \rightarrow BrO + O_2 \quad (7)$$

$$Cl + O_3 \rightarrow ClO + O_2 \quad (8)$$

Those chlorine- and bromine-bearing compounds from human-made CFCs do not interact directly with O_3 but provide a surface for chemical reactions [Köhler et al., 2010]. However, not all the processes affecting both sulfur aerosol elimination and formation are full understood yet.

To analyse the processes of the tracers, it is necessary to know their most important chemical reactions and possible sources besides VA plumes. The capability to distinguish volcanic from anthropogenic tracers is substantial for the analysis. Not in every case can an enhanced concentration measurement of a certain volcanic tracer be allocated with certainty to the VA plume. The strong influence of other sources - mainly man-made – has to be taken into consideration.

3 Data and Models

After a short overview on Metair (airborne measurements) and NABEL (ground based sites), the data selections for the three theses are presented including the applied measurement systems for those aerosols and gases mentioned in chapter 2. Also the setup of two dispersion models (HYSPLIT and FLEXPART) will be introduced shortly. They model the path of the air parcels reaching Switzerland on several altitudes and are therefore helpful to analyse the meteorological situation for the reconstruction of chemical and physical processes.

3.1 Metair

Metair delivered the first Swiss *in-situ* measurements of the VA plume in spring 2010. Details about the vertical and horizontal extent of the ash cloud allowed BAZL to decide whether an airspace closure might be appropriate or not. Measurement flights were performed on 17, 18 and 19 April (closed airspace), 9 and 18 May (open airspace).

Metair operates economic aircraft for scientific research studies since 1990 [Neininger et al., 2001]. The recent Metair research aircraft is a touring motorglider (Diamond Aircraft HK36 TTC-ECO, also referred to as DIMONA, figure 4) carrying several instruments in the fuselage and underwing-pods. The operation altitude is up to 6000m with an average cruise speed of 180 km h-1. Additionally, its soaring capability makes it suitable to directly investigate VA plumes which might cause engine failures. This risk is however low due to the piston engine. By the time of the eruption of Eyjafjallajökull, the measuring system was configured for a CH4-study in Switzerland which allowed a quick instrumentation-adaptation for the VA plume. Beside many other parameters, also true air speed, position and altitude, windspeed and inlet misalignment angle are recorded during the flight. This allowed a precise validation of the gathered data.

Figure 4: Preparing Metair Dimona for a research flight on 19 April 2011. The two underwing pods carry the measurement devices to collect volcanic data (picture: Metair).

3.2 NABEL

The Swiss Air Quality Monitoring Network (NABEL) is a joint project of the Federal Office for the Environment (BAFU) and the Swiss Federal Laboratories for Material Science and Technology (EMPA). NABEL operates 16 air pollutant measurement sites covering different immission types (urban, rural or remote) as well as several topographic height levels [EMPA, 2010]. Due to the continuous time series measurement of parameters, these ground measurements provide additional information to complement Metair flight results. Some of these sites were selected (Figure 5, upper image) to compare their measurement values with those of Metair. Measurement sites were chosen according to their measurement programm [Empa, 2010] and roughly cover the area of the flight path tracks. Lugano was enclosed to provide additional information about the southern alpine side.

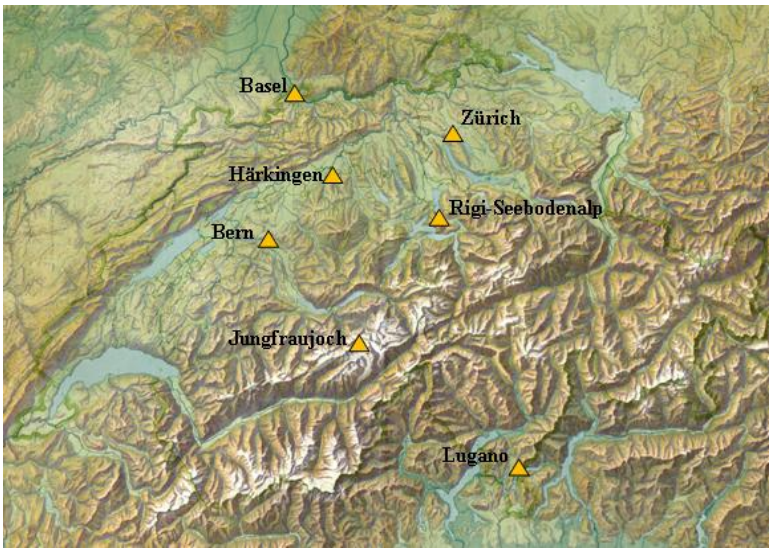

Selected NABEL sites (m AMSL)	Immission type	Atmospheric Layer
Basel BAS(317 m)	suburban	PBL
Bern BER(536 m)	urban (main road)	PBL
Härkingen HAE(431 m)	rural (next to highway)	PBL
Jungfraujoch JFJ(3578 m)	mountain	mostly FT
Lugano LUG (281 m)	urban (park)	PBL
Rigi-Seebodenalp RIG(1031 m)	rural (elevated)	FT/ PBL
Zürich ZUE(410 m)	urban (park)	PBL

Figure 5: Locations of the selected NABEL sites (background image: http://www.reliefs.ch/kartopro.htm, access: 7. June 2011), immission types and atmospheric layer (PBL: planetary boundary layer, FT: free troposphere).

Basel, Bern, Härkingen, Lugano and Zürich are situated within the planetary boundary layer (PBL) in strong polluted urban or more rural areas (figure 5), whereas the two elevated sites occasionally (Rigi-Seebodenalp) or mostly (Jungfraujoch) log values of the free troposphere (FT), which occurs especially during summer nights and winter month. In fair weather, both Rigi and Jungfraujoch are more or less influenced by thermally induced injections of the PBL pollutants [Henne et al., 2004]. Since Jungfraujoch is the most remote measurement site in Switzerland, it therefore delivers the most accurate ground-data regarding VA plumes.

3.3. Lagrangian models

To receive an idea of the distribution pattern within Switzerland as well as an image of the VA plume trajectory and travel time, Lagrangian models are powerful instruments to model atmospheric transport. Opposed to Eulerian models which use grid cells that are fixed in place, the Lagrangian view offers an alternative perspective that focuses on movement and uses an object-based approach.

A recent indication of the tremendous economic importance of Lagrangian models was their role in predicting the spread of volcanic ash from the eruption of Eyjafjallajökull [Lin et al., 2011]. HYSPLIT and FLEXPART simulate foreward/backward trajectories for air parcels and the atmospheric dispersion of particles respectively. Different configurations regarding for- or backward calculations, atmospheric input data, etc. can be adjusted for both models. Also flight planning for research aircrafts were supported by consideration of forward trajectory charts [Schumann et al., 2010]; Neininger, 2010].

3.3.1 HYSPLIT

The HYSPLIT model (Hybrid single particle Lagrangian integrates trajectory model) was developed by National Oceanic and Atmospheric Administration (NOAA). HYSPLIT computes simple air parcel trajectories (figure 6) as well as complex dispersion and deposition simulations. At first, this was a joint project between NOAA and the Australia's Bureau of Meteorology (BAM) before a number of various contributors enhanced HYSPLIT with improvements in advection algorithms, updated stability and dispersion equations. The HYSPLIT model can be run interactively on the website of NOAA (URL: http://ready.arl.noaa.gov/HYSPLIT.php). Different models such as for trajectories, dispersion and volcanic ash using different meteorological data can be chosen and applied by the user [Draxler and Rolph, 2003].

For the analysis of Eyjafjallajökull airmasses reaching Switzerland, two HYSPLIT options were used. For the HYSPLIT backward trajectories model, the end date and time were roughly adjusted to the take off time of Metair research flights. Thus, the *in-situ* measure-ments of the air layers could be allocated to its path and point of origin. The following para-meters were defined: trajectory ending levels (1500m, 3500m and 4500m AMSL); target-area: LSZB (airport Bern-Belp); vertical motion: model vertical velocity; duration: 48 to 120 hours (depending on the windspeed); meteorological data: GDAS (Global Data Assimilation System); other parameters: default (figure 6).

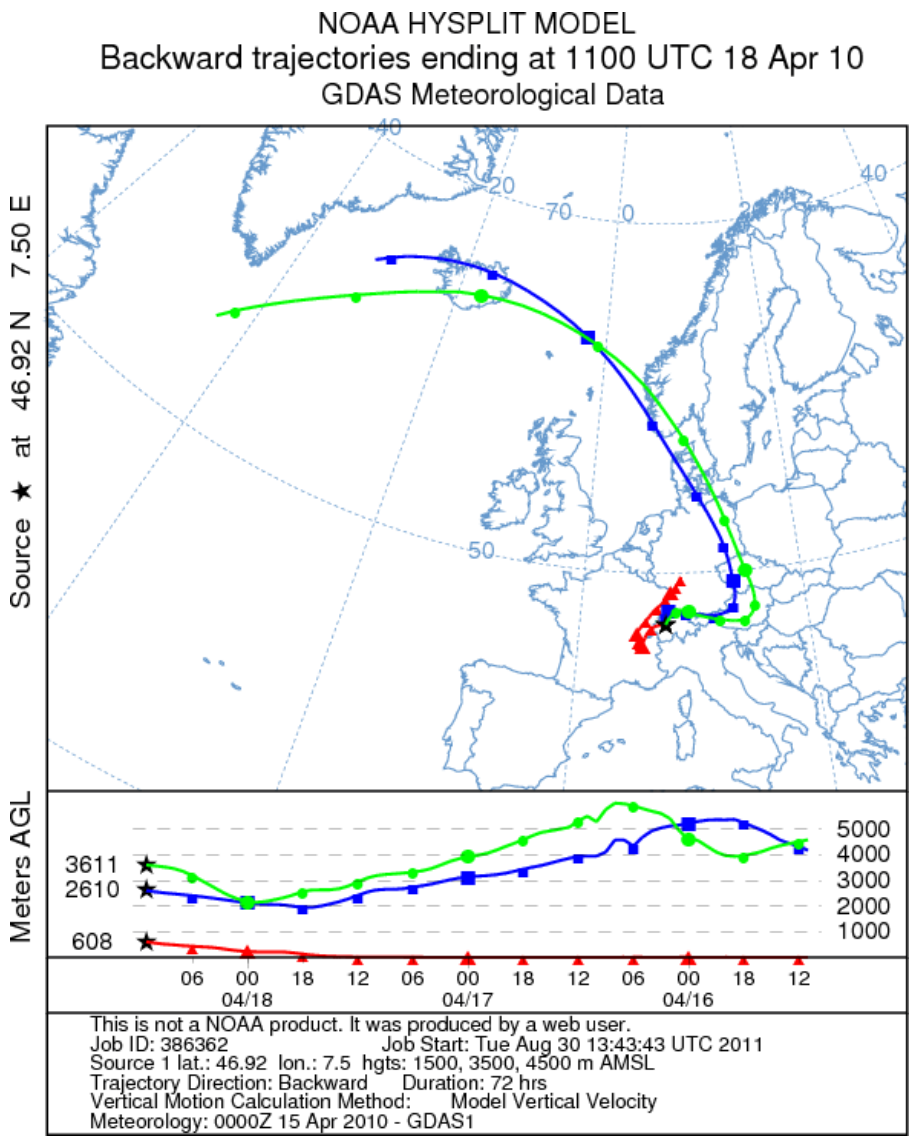

Additionally, a volcanic ash dispersion model can be applied interactively. For each flight day, the dispersion pattern for several flight levels (FL) was calculated (surface-FL550; surface-FL200, FL-200-FL350, FL350-FL550). The following settings were defined: source position and volcano summit height; runtime duration and hours of eruption: 48 hours; concentration level: 2; ash reduction: small (for the europeanwide fair weather in April phase) and medium (for the humid synoptic situation in May), Ash column top: 21'000 to 30'000 feet; other parameters: default.

Figure 6: Interactive Output of NOAA HYSPLIT model for 72h backward trajectories for 18 April 00 UTC with the target area LSZB (airport Bern-Belp) and GDAS (Global Data Assimilation System) meteorological input data. Heights of three defined trajectory-ending levels over Bern were set at 1500m, 3000m and 4500m AMSL. Air parcels at middle (blue) and higher altitudes (green) originated from Iceland and therefore likely contained VA (source: ready.arl.noaa.gov, access: 30 Aug 2011).

3.3.2 FLEXPART

FLEXPART is a Lagrangian particle dispersion model (LPDM) developed at the Norwegian Institute for Air Research in the Department of Atmospheric and Climate Research. FLEXPART has been designed for calculating long-range and mesoscale dispersion of air pollutants from point sources. Usually, FLEXPART uses meteorological fields from the ECMWF numerical weather prediction model [Stohl et al., 2005]. On behalf of national authorities, first simulations of the VA plume have been set up by

EMPA already one day after the first eruption (figure 16). NCEP/GFS forecasts were used to simulate the particle dispersion. Among other information, these outputs served BAZL as a basis of decision for airspace closures. According to Bukowiecki et al. [2010], Met Office UK operates NAME, a Lagrangian air pollution dispersion model similar to the FLEXPART model. The current version NAME III attracted worldwide attention during the eruption of Eyjafjallajökull providing basis for the VA plume dispersion charts by the Volcanic Ash Advisory Centre (VAAC, see appendix A).

For this analysis, also some plots of EMPA were studied besides own versions (URL: http://transport.nilu.no/browser/fpi). Different projects (several volcanic eruptuions, Fukushima, etc.) can be chosen by declaring the event, time span, age class of tracers, gridbox or segment line for horizontal or vertical pots (other settings: default). This has been compiled for several segments, boxes and time spans during Mid April and May 2010. As Iceland is located in the middle of the North Atlantic, the weather is strongly influenced by cyclonic activity along the North Atlantic storm tracks. Although depressions are more frequent and deeper in winter, they still have an impact on Icelandic weather in other seasons, often with frequent changes in windspeed and direction [Petersen, 2010]. However, the eruption of Eyjafjallajökull happened during a period of an anticyclonic system over Northern Europe and Northern Atlantic with its core south of Iceland. This was the case for both surface and 500mbar geopotential level.

3.4 Data selection for tracer analysis

For the analysis of tracer correlation, ground based measurements of the gas and aerosol phase at the selected NABEL sites (BAS, BER, LUG, RIG, ZUE, HAE, JFJ) were applied.

- **Gas phase**

In a first step, specific NABEL parameteres are chosen for a detailed tracer correlation to analyse the relationships between thre tracers. On one side, SO_2, CO_2, CO, NO_2 and O_3 components of the gas phase are analysed. NABEL measurements of CO_2 are conducted by an infrared absorbtion principle (LICOR Li-7000, Picarro G301), CO by non-dispersive infrared absorption (Horiba AMPA360 and 370), O_3 with UV-absorption (Thermo 49C and 49i), SO_2 by using the UV-fluorescence method (Thermo 43C TL and 43i TLE) and NO_2 by the intensity of chemoluminsence radiation (table 3).

- **Aerosol phase**

For a detailed image of the particle size distribution, also measurement data of optical particle counters (OPC) and scanning mobility particle sizer (SMPS) were examined. Whereas OPC-data is used for the larger aerosol fraction (D_{opt} >0.5µm), SMPS-data measures the smaller fraction more precisely. Therefore, a combination of both data served for an appropriate aerosol size distribution. This detailed size distribution insight allows correlation calculations with specific aerosol sizes compared to the broad band of PM10 aerosol sizes.

Aerosol size distribution:

OPC Grimm dust Monitor: The measurement principle of the light scattered by the particles and then converted into particle size relies on the Mie-theory [Justus-Bichler, 2006]. This OPC measures optical diameters from 0.3µm - 20µm in the following 15 bins: >0.3µm, >0.4µm, >0.5µm, >0.65µm, >0.8µm, >1µm, >1.4µm, >2µm, >3µm, >4µm, >5µm, >7.5µm, >10µm, >15µm and >20µm. Only particles <40µm (dependent on wind and flux) are capable to enter the inlet. The instrument has a temporal resolution of 6 seconds. Previous to the measurement flights, this OPC was compared with an identical Grimm dust monitor model at Jungfraujoch and results were empirically corrected afterwards [Bukowiecki et al., 2010]. Grimm measurements can also serve in terms of aerosol concentrations by summing up several bins, which was the case for the May phase of Metair.

Scanning mobility particle sizer: Additional to the Grimm dust monitor, Jungfraujoch operates a spectrometer to size number concentrations without assuming the shape of the particle size distribution. Compared to OPCs, this scanning mobility particle sizer (SMPS TSI 3034) is independent of the refractive index of the particle or fluid, and has a high degree of absolute sizing accuracy and measurement repeatability [TSI, 2011]. The SMPS at Jungfraujoch measures mobility diameters (D_{mob}) between 10 and 350 nm using a combination of differential mobility analyser (DMA, TSI Inc., Model 3071) and a condensation particle counter (CPC, TSI Inc., Model 3775) [Jurányi et al., 2011]. Basically, entering aerosols are classified according to electrical mobility inside the DMA, and only those inside of a narrow range of mobility exite through the output slit where their concentration is determined in the CPC.

Aerosol mass concentration

A **combination of a gravitational method and a HIVOL (high volume) instrument** (Digitel DA 80H) is applied to retrieve particulate matter (PM10). Particle concentration can be derived by weighing a filter before and after the passage of a determined air volume [BAFU, 2010]. This occasional measurement is completed with a continuous, real-time measurement with Thermo Electron FH 62 l-R and Thermo Scientific TEOM 8500 FDMS (beta radiation principle; Tapered Element Oscillating Microbalance) [EMPA, 2010].

3.5 Data selection for meteorological analysis

Both NABEL and Metair delivered data for the analysis of the weather influence on gas and aerosols.

- **Gas phase**

All available gas phase data were used for this section. The above mentioned measurement methods for the gas phase by NABEL are similar to the Metair methods (table 3). The airborne measurements

of some volcanic gas substances such as CO_2 and H_2O have been carried out by a differential infrared gas analyser (IRGA). Its concept is based on determining the absorption of an emitted infrared light source through a certain air sample. CO was identified by a resonance-fluorescence radiation method in vacuum UV-range (Aerolaser AL-5003), O_3 by UV-absorption of a PSI development of a former Monitor Labs device), and NO_2 by an in-house development (Metair-NoxTOy) using a 6-channel luminoldetector. CO, CO_2, NO_2, O_3 and relative humidity were recorded on most days. SO_2 was not measured quantitatively by Metair.

- **Aerosol measurements**

Additional to NABEL OPC data, also Metair OPC data(MetOne and an identical Grimm dust Monitor as the instrument type on Jungfraujoch) served for the investigation the aerosol phase. Also condensation particle counters deliver aerosol numbers at all selected NABEL sites.

Table 3: Measurement methods and instruments of Metair and NABEL and measurement sites of the specific tracers for the meteorological analysis (sources: Neininger, 2009, Metair website, EMPA, 2010).

Tracer	Metair measurement methods	Metair instruments	Tracer	NABEL measurement methods	NABEL instruments	NABEL sites
Aerosols	Optical particle counter - 2 bins; Optical particle counter - 15 bins	MetOne OPC 4903; Grimm dust monitor 1.108	**Aerosols**	Condensation particle counter, combined method	CPC TSI 3775A, 3022A; Digitel DA 80H	All sites
H_2O	Differential infrared gas analyser; relative Humidity	LICOR- IRGA LI-6262; LI-7500	**SO_2**	UV-fluorescence	Thermo 43C TL, Thermo 43i TLE	BAS, HAE, JFJ, LUG; RIG, ZUE
CO_2	Differential infrared gas analyser	LICOR- IRGA LI-6262 and LI-7500	**CO_2**	Infrared absorption principle	LICOR LI-7000, Picarro G301	HAE, LUG
CO	Resonance-fluorescence method	Aerolaser AL-5003	**CO**	Non-disp. Infra.-absorbtion	Horiba AMPA360, Horiba AMPA370	BER, HAE, JFJ, LUG, RIG
O_3	UV absorption	PSI development	**O_3**	UV-absorption	Thermo 49C, Thermo 49i	All sites
NO_2	6-channel luminol-detector	Metair NOxTOy	**NO_2**	Chemiluminescence-radiation	Horiba ABNA 360/370; Thermo 42i TL, eco Physics CLD 89p	HAE, LUG, ZUE

- **Aerosol number and size distribution**

MetOne OPC (Model 4903 Hach Ultra Analytics Inc., ISA) measures the number of aerosols in two bins with an optical diameter range of D_{opt} >0.3µm and D_{opt} >0.5µm respectively. This type of OPC uses a laser diode light source and collection optics for particle detection. The collection optics collects and focuses the light scattered by the particles onto a photo diode that converts the bursts of light into electrical pulses. The pulse height corresponds to the aerosol size. Pulses are counted and their amplitude is measured for aerosol sizing [Hach, 2004]. MetOne was calibrated by using polystyrene latex spheres (PLS) and measures with a 1 second temporal resolution. Metair aerosol data were post-processed by PSI (Bukowiecki et al., 2010].

Condensation particle counter (CPC 3775A and 3022A) is an optical device to measure aerosol number by means of scattered light. In a first step, air gets saturated by the steam of

a specific liquid. The saturated air will then be cooled inside a condensator which results in a supersaturation and thus condensates on the surface of the aerosols. This increase in size enables the aerosol to be recorded optically. A sufficient large aerosol crossing the laser beam generates scattered light recorded by a detector [EMPA, 2010].

- **Meteorology**

To analyse the synoptical and mesoscale weather situation and wind distribution, diverse sources were used (e.g. radar and Eumetsat satellite images (both provided by Meteotest), Payerne soundings, wetter3.de and FLEXPART model outputs.

3.6 Data selection for ageing and chemical processes

- **Ageing processes**

The development of VA plumes within Switzerland was investigated by examining ground based SO_2 and PM10 measurements with the above mentioned measurement methods. Additionally, also HYSPLIT outputs were considered to analyse the source of the swiss airmass as well as the trajectory length defining the settlement time of larger particles.

- **Chemical processes**

The O_3 depletion phenomenon was examined by comparing ground based O_3 and SO_2 data. The same parameters were considered within Metair research flight profiles.

4 Results and discussion

Measurements carried out by Metair and NABEL cover different temporal and spatial scales. Whereas ground based measurements deliver continuous time series of the parameters, Metair shows single footprints with a high horizontal and especially vertical resolution of VA *in-situ* measurements enabling detailed cross-sections of the atmosphere. Measurement flights have been performed from 17 – 19 April as well as on 9 and 18 May, thus those days are investigated thoroughly in combination with NABEL measurements. This chapter contains airborne and ground based measurement results, tracer correlation, meteorological analysis as well as a detailed insight into ageing and chemical processes according to each theses defined in the introduction.

4.1 Airborne measurements

Metair performed several flights primarily across the Swiss Plateau and Prealps with varying altitudes up to a maximum of 6000m AMSL. For each day, a continuous ascent up to at least 5000m AMSL was chosen to compile an atmospheric profile. The main focus for Metair measurements are concentrations for aerosols >0.3µm optical diameter (Aer03) and >0.5µm optical diameter (Aer05) as well as other suitable tracers (CO, CO_2, O_3 and relative humdity).

April event

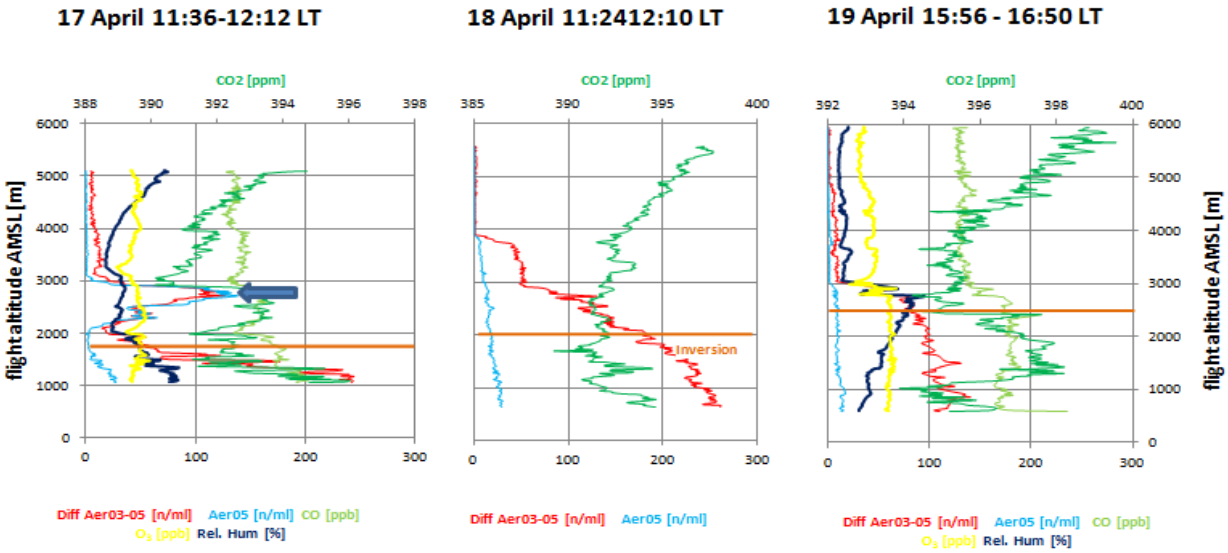

Figure 7: Vertical Metair profiles of three flights during April phase. The light blue and red lines indicate particle concentrations between 0.3-0.5µm (Diff Aer03-05) and >0.5µm (Aer05), respectively. CO_2, CO, O_3 mixing ratios and relative humidity are outlined, as well as the inversion altitude (data: Metair).

During the three consecutive days in April, strongest aerosol peaks were recorded at 17 April at an altitude just below 3000m AMSL (figure 7, blue arrow). This is also clearly visible on the Google map including the projected flight path and its respective concentrations (see appendix A). Aer05 number concentrations reached maximum values of 140 particles cm^{-3}. CO and CO_2 likewise show slightly increased values at the same altitude. On the subsequent days, the signals faded out without indicating new arriving distinct plume layers. The largest values between the surface and the inversion altitudes can be explained by the presence of anthropogenic pollution in the PBL and cannot be directly allocated to the VA plume.

May event

The two measurement days in May strongly differed in terms of aerosol and gas concentrations. Tracer signals on 9 May remained within the range of background concentration (figure 8). On 18 May, the situation looked completely different except the considerable high relative humidity up to approx. 3300m AMSL. Largest aerosol concentrations were measured at 3600m AMSL. Especially the number of aerosols between 0.3 and 0.5µm are strongly increased. A possible reason is the enhanced formation of accumulation mode particles (appendix A) by the conversion sulfur dioxide into sulfates [Bukowiecki et al., 2010]. Whereas CO_2 and CO values grew within the VA layer, O_3 dropped distinctly at the same level. NO_2 values are not displayed for both months as they are not reasonable.

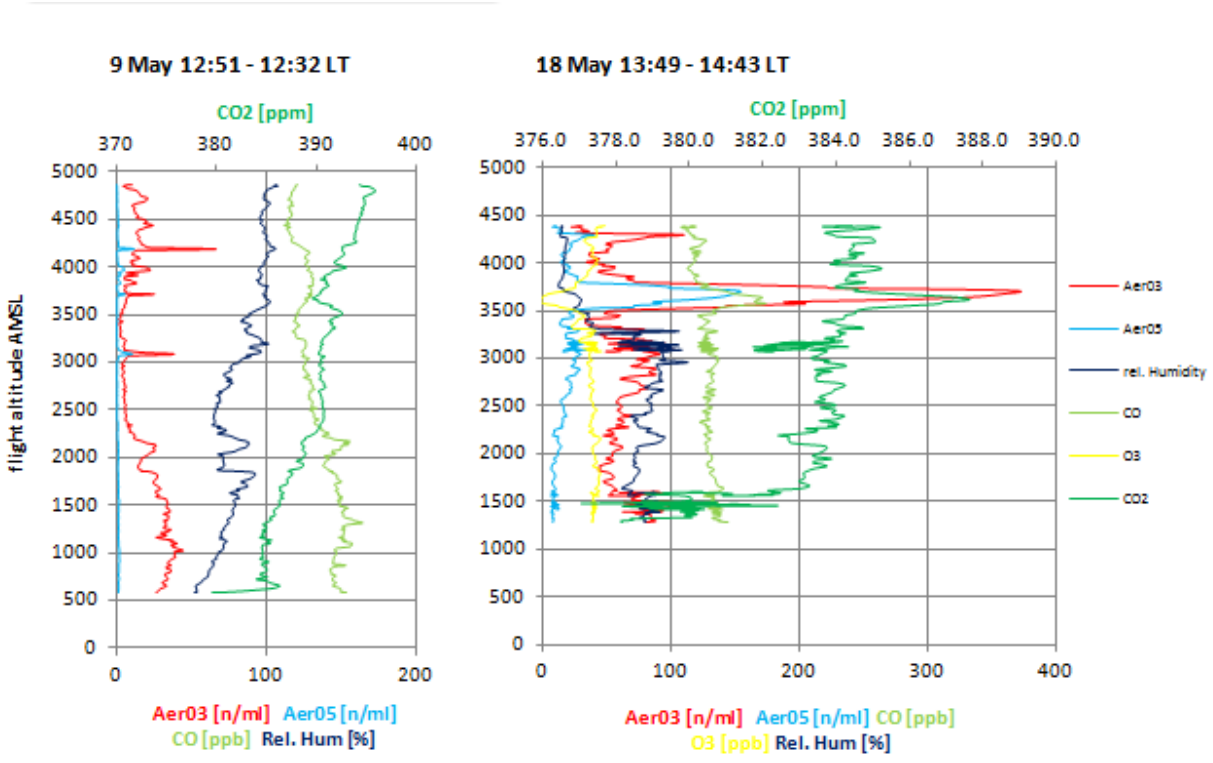

Figure 8: Metair vertical profiles of 9 May between 12:51 and 12:32 LT and 18 May between 13:49 and 14:43 LT.

4.2 Ground-based measurements

The analysis of NABEL tracers is subdivided into the two eruption episodes in April and May and a distinction between the remote, mostly PBL-unaffected high-level site at Jungfraujoch and the other sites at lower levels. Except Rigi, it is likely that measurements of lowland sites are masked by anthropogenic pollution for most periods.

April phase

Jungfraujoch: The arriving VA layer was first indicated by a simultaneous significant increase in PM10 and SO_2 at Jungfraujoch in the evening of 17 April (first peaks around 16 April 10 LT at low-lying measurement sites are negligible as the VA layer was about to arrive earliest one day later). Both tracers increased significantly by a factor 3 (PM10 increase from a background concentration of approximately 5µg/m^3 to a maximum value of 14µg/m^3) up to factor 10 (SO_2 increase from a mean concentration of 0.04ppb to 0.4ppb) around 20 LT (figure 9). A second peak with the highest measured values at Jungfraujoch during April phase was recorded at 18 April shortly around 16 LT. By this time, both PM10 and SO_2 reached their maximum value with 32µg/m^3 and 3ppb, respectively. On 19 April, concentrations of both tracers peaked at approximately 12 LT before SO_2 decreased constantly to a normal level. PM10 remained on an increased level until 21 April (figure 13).

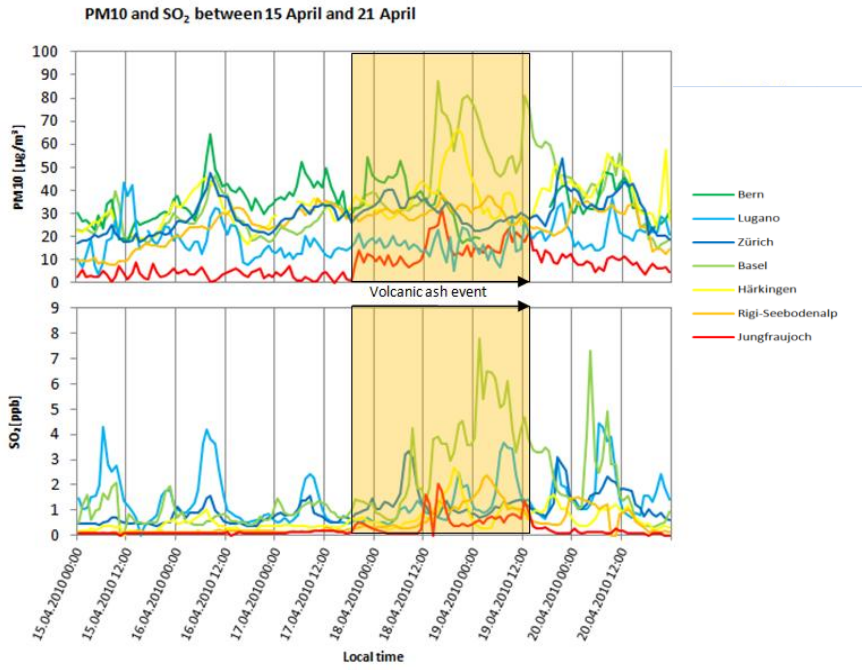

Figure 9: PM10 and SO_2 between 15 April 0:00 LT and 21 April 0:00 LT at selected NABEL sites. The orange area shows the time span of the VA plume within Switzerland (data: NABEL (BAFU and Empa)).

Other measurement sites: At the same time the first plume arrived at Jungfraujoch, also other sites recorded changes in tracer concentrations. The first significant increase in PM10 was measured in Basel (25% increase) in the evening of 17 April, whereas its respective SO_2 values remained almost on the background level. Also Härkingen and Zürich measured slight PM10 increases with more or less constant SO_2. PM10 in Bern built up quickly as well, but as the background concentration is generally high and SO_2 values are not recorded, this increase cannot be assigned with certainty to the VA plume. Measurements at Bern, Härkingen and Zürich are therefore

probably more influenced by anthropogenic emissions. Lugano and Rigi revealed no remarkable amplifications regarding both tracers. On 18 April 15LT, Basel showed again some increase in SO_2 (4.1ppb at 15 LT) by a factor 5 (annual average: 0.8ppb). Simultaneously, PM10 values increased to 87µg/m^3 (annual average: 16.2µg/m^3). The increase in aerosol concentration is also visible in overall number concentrations (see appendix A). Other NABEL sites measured only the enlarging of just one tracer at a time. The following day all the selected sites showed modest increases of both tracers at the same time, which points out the presence of volcanic airmasses. Rigi was the first NABEL site detecting the VA plume on 19 April around 3 LT (only small increase of both tracers), followed by Lugano (9 LT), Basel (12 LT), Härkingen and Zürich (both sites around 20 LT; see figure 13). Generally spoken, none of the low- and mid-level NABEL sites except Basel recorded nearly the same increase factor of tracers as Jungfraujoch did, which might be mainly due to the down-mixing, PBL-processes and the commonly higher background concentration.

Besides the above analysed tracers, also CO, CO_2, O_3 and NO_2 measurements have been accomplished. Comparing the previously mentioned increase in SO_2 and PM10 with CO and NO_2 of Härkingen (no values of Basel available), shows that only NO_2 has some irregular patterns at the same time, in contrast to the regular cycles on the preceeding days, which are however not unusually extreme. CO mass concentrations do not reveal any remarkable alterations. The amplitudes of all sites seem to remain within the background noise level. High-alpine Jungfraujoch shows almost no variations, whereas the diurnal cycle is clearly indicated at the polluted low-level sites. Although the daily peak in the early morning is constantly rising from 17 April on, this phenomenon cannot be directly connected to the arriving VA plume as peak values were already higher in subsequent weeks. Jungfraujoch values stagnated between 393 and 395ppm. Also O_3 signals persist

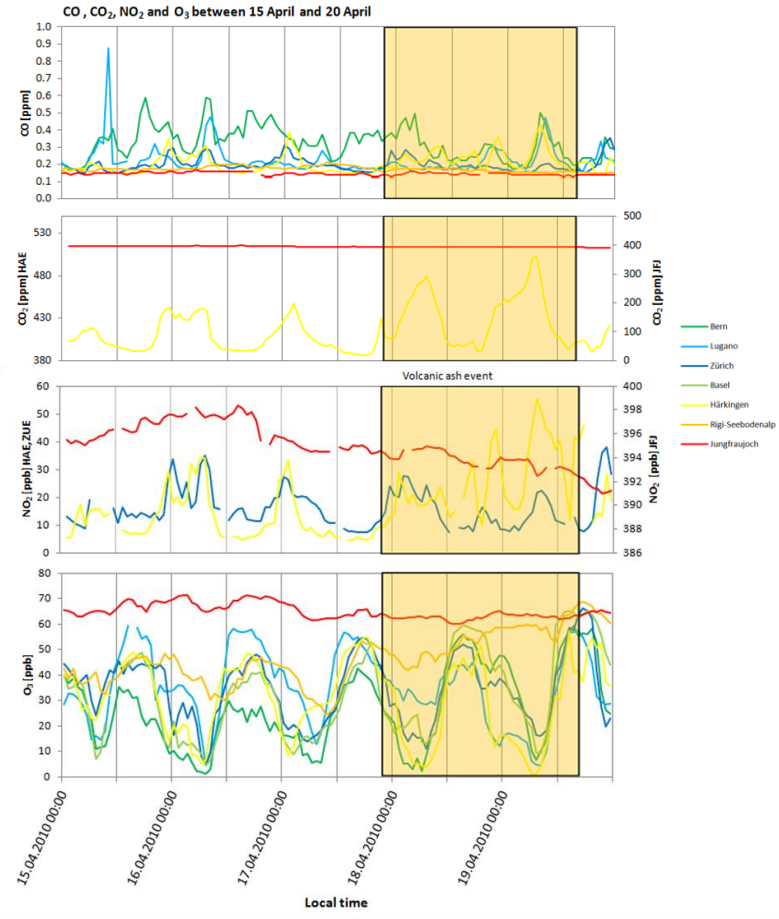

Figure 10: CO, CO_2, O_3 NO_2 and O_3 measurements in the phase between 15 April and 20 April 0LT (data: NABEL (BAFU and EMPA)).

within the noise. The expected decrease within a VA layer is not clearly present at any of the measurement sites (figure 10).

May phase

Jungfraujoch: PM10 measurements did not peak clearly on 9 May but show a generally higher concentration with local maximas around 8 LT and 17 LT. SO_2 values were also highest around 8 LT and then quickly decreased to the normal background concentration level. On the last research flight day at 18 May, Jungfraujoch recorded the highest tracer concentrations of the entire eruption phase of Eyjafjallajökull. PM10 strongly increased to a maximum of 69µg/m^3 and also the SO_2 signal was much higher than in the April phase and increased to 12ppb. Both tracers increased gradually in the afternoon reaching their maximum at 20 LT (figure 11).

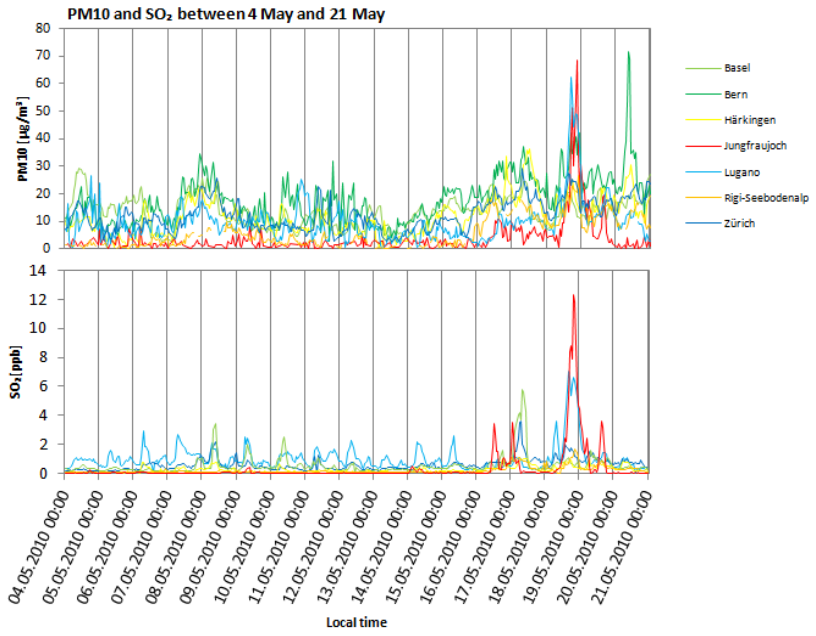

Figure 11: PM10 and SO_2 measurements between 4 May 0:00 LT and 21 May 0:00 LT at selected NABEL sites (data: NABEL (BAFU and Empa)).

Other measurement sites: The only site recording a simultaneous increase of both tracers on 9 May was Basel with maximums between 5 to 7 LT. Other measurement sites disclose some factor 2-4 SO_2 increases at 0 LT (Zürich, Rigi) and from 6 to 9 LT (Lugano), but only vague changing PM10 concentrations. This was not the case for 18 May. During the afternoon, most selected NABEL sites recorded rising PM10 signals with their maximums around 15 LT (Basel, Zürich), 19 LT (Lugano) and 21-22 LT (Härkingen, Rigi). In comparison to the well matching simultaneous increases of both tracers in the April phase, the respective SO_2 concentrations on 18 May did mostly peak a bit earlier than the respective PM10 values. The strongest signal on 18 May (besides Jungfraujoch) was measured in Lugano with a SO_2 peak of 7.1ppb and a PM10 maximum of 62µg/m^3 (figure 11). On the other hand almost no increased CO, CO_2, O_3 and NO_2 values were present at ground based sites during the measurement flight days in May (appendix A). Regarding the different CO background concentrations, only Lugano shows a slightly higher signal on 18 May. In terms of O_3 only a small decrease at Jungfraujoch (-10% at 9 May at 8 LT) was measured, which is questionable to refer to the VA plume.

4.3 Tracer analysis

In order to investigate the relations between the tracers, parameters at Jungfraujoch (most representative measurement site for the free troposphere within Switzerland) are analysed in terms of correlation, as the presence of a simultaneous increase of two volcanic tracers is likely to indicate an airmass coming from Iceland.

Table 4: Correlation coefficient (first line), P-value (second line) and number of samples (third line) for each tracer at Jungfraujoch in the VA phase from 17 April 00 LT to 20 April 00 LT, data: NABEL (EMPA and BAFU).

	PM10	NO_2	CO_2	CO	O_3
SO_2	**0.752** 0.0000002 71	**-0.495** 0.0000214 68	**-0.475** 0.0000569 67	**-0.491** 0.0000191 70	**-0.318** 0.00698 71
PM10		**-0.303** 0.0116 69	**-0.659** 0.0000002 68	**-0.265** 0.0256 71	**-0.197** 0.0969 72
NO_2			**-0.0318** 0.801 65	**0.307** 0.0111 68	**0.318** 0.00801 69
CO_2				**0.438** 0.000206 68	**0.0237** 0.847 68
CO					**0.00595** 0.961 71

As none of the parameters are normally distributed, a Spearman correlation test is applied. According to the correlation coefficients (strong if > 0.8) and p-values (no significant relationship between the tracers if p-value < 0.05), only PM10 with SO_2 show a nearly strong positive correlation, whereas the other tracers do only show weak or even negative relations (table 4). It is likely that CO, NO_2 and CO_2 originate from an anthropogenic source during April phase, which is also indicated in the April profiles of Metair (figure 7), whereas the signals of SO_2 stems most probably from the VA. Thus, SO_2 depicts the best tracer for the gas phase. Taking a closer look on the volume concentration of different particle sizes (figure 12), a bimodal distribution with the first peak in the accumulation mode (0.2-0.3 µm) and coarse mode (around 3 µm) can be detected for both April and mid May phase. Whereas for the April phase, the correlation between SO_2 and $D_{2.9}$ is clearly best (> 0.9), PM10 correlates best with SO_2 for the May phase. For a general VA overview across different meteorological conditions, PM10 is more representative, as none of the specific particle sizes shows a constant correlation. Within the free troposphere, PM10 depicts therefore the best tracer in terms of particles, whereas SO_2

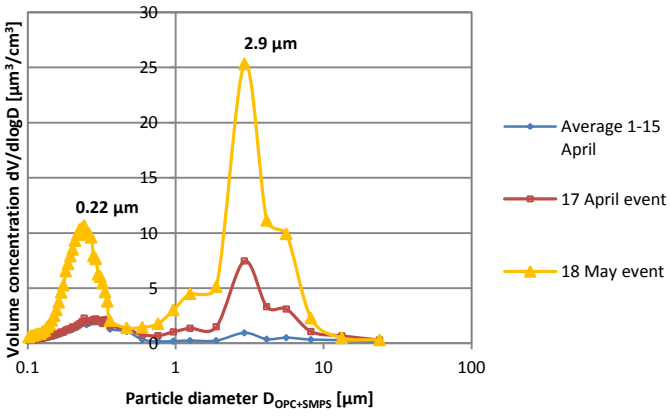

Figure 12: Volume concentration of different particle sizes (symbols) at Jungfraujoch by a combination of SMPS data (D <0.5µm) and OPC data (D >0.5µm). Non-VA phase: 1-15 April, 17 April event: 19-23 LT, 18 May event: 1-23 LT; data: NABEL (BAFU and Empa).

represents the most applicable indicator for the presence of a VA layer referring to the gas phase particles [Hüglin et al., 2010; Bukowiecki et al., 2010]. This relation is emphasized by also comparing the correlation of SO_2/PM10 during non-volcanic phases (correlation: 0.24) with volcanic events (> 0.73). Thus, this tracer combination (within FT) most likely only correlate when VA arrives and is therefore the most valuable indication for its presence.

4.4 Comparison of measurements with meteorology

Thesis: Characteristics of the particle and gas phase depend on precipitation and humidity, winds and atmospheric stratification. Rain is expected to increase the scavenging processes and wash out of aerosols. In weak wind conditions, less particles of the large fraction reach Switzerland as they have more time for gravitational settling between Iceland and Switzerland. Stable atmospheric stratification lead to increased concentration values within PBL because of reduced mixing processes with the FT.

To assess the influence of meteorological conditions on the VA plume, each volcanic ash cloud event in Switzerland, with days on which research flights were performed (mid April, early May, mid May), is analysed on the mesoscale and the synoptic level and compared with the measurements.

4.4.1 April event

- **Meteorological situation**

  Europe: Regarding the duration of the air masses drifting towards Central Europe on 17 April (first research flight), it is necessary to take a closer look on the European meteorological conditions starting on 15 April. On this day, westerly to northwesterly upper level winds in the North Atlantic region were moderate to strong (18-29ms^{-1} at 3km and 32-44ms^{-1} at 5km altitude) compared to the lower windspeeds at the surface. The respective airmass first migrated in a southeasterly direction towards Norway (figure 13) before it spread towards Sweden, Great Britain and Ireland. During the subsequent days, the high pressure zone above Eastern Europe moved towards the Black Sea resulting in a northeasterly current in Central Europe.

  Switzerland: Southwards of the above mentioned westwind zone over Iceland, a high pressure ridge reached from Northern Atlantic to Germany and Austria. This synoptic situation led to mostly fair weather on the northern side of the Alps between 17 and 19 April. The southern side received more humidity and was partly cloudy due to a low pressure system over Northern Italy. Local showers of rain occurred mainly in the south and occasionally along the Alps and Prealps (NABEL data from Lugano and Rig-Seebodenalp: <5mm per day, see appendix B). Strong easterly to northeasterly winds became slightly weaker during the next days and veered off to a more westerly direction. Inversions and

isotherms situations occurred on each day raising its lower limit from 1200m to 2000m AMSL. Its upper limits can be seen well on the pictures taken by Metair (figure 14).

- **Comparison with measurements**

  According to NABEL data, the first conclusive indications for the presence of a VA plume were the rising values of PM10 and SO_2 on Jungfraujoch in the evening of 17 April. The Metair research flight in the afternoon confirmed NABEL measurements with maximum particle concentrations above 3000m AMSL. A new plume arriving from Germany was first measured starting with strong signals in Basel in the afternoon of 18 April (also clearly visible by a significant rise of aerosol number concentration by a factor 5, see appendix A), and followed by Härkingen (evening of 18 April). On the last day of the April episode, finally 4 of 7 sites recorded marginally increased values during the whole day (Rigi, Lugano, Basel, Härkingen and Zürich) which is likely to originate from subsidence and ongoing dilution of the first VA layer. The above mentioned second VA layer was also detected by Jungfraujoch in

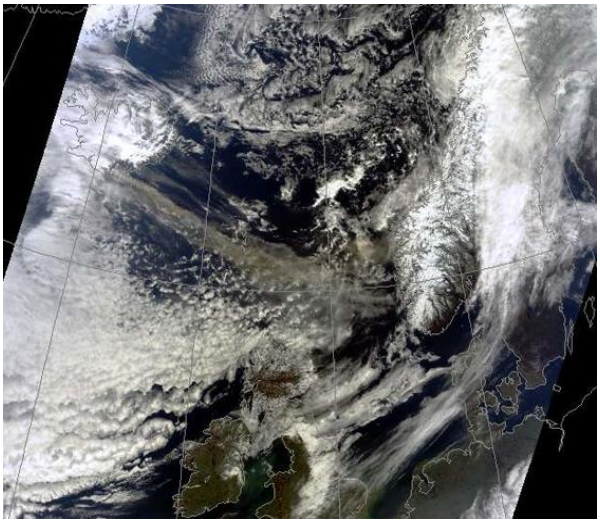

Figure 13: MODIS image from 15 April 2010 11:30 UTC. The southeastward spreading plume drifting towards eastern Norway is clearly visible. (source: Nordic Volcanologic Center).

Figure 14: Upper level of inversion taken from Metair Dimona at 17 April 13:01 LT at a flight altitude of approximately 3200 AMSL (source: Metair).

the afternoon of 18 April as well as a third faint plume at noon of 19 April. Both measurements correspond well to the research flights with noticeable increases of values at higher altitudes. However, the analysing of all selected NABEL sites show that only Jungfraujoch and Basel logged clear increases of both tracers during the April phase.

The sequence of enhanced PM10 and SO_2 tracers reach a good agreement with the meteorological conditions during these three days. Jungfraujoch was at first influenced by southeasterly winds transporting increased tracer concentrations westwards across northern Switzerland. During the subsequent days, winds turned west to northwest and the prevalent anticyclonic system led to a continuous subsidence of airmasses. Both resulted in the

advection of a polluted layer approaching Switzerland from northwest (figure 15) and was unambiguously observed in Basel. The effect of the subsidizing airmasses on 18 and 19 April arises on the Metair profiles by indication of concentration dilution. On 19 April, the layer is not recognizable anymore in the Metair profiles due to down-mixing into the PBL. Regarding 18 April (moderate CAPE) and 19 April (low CAPE) in terms of precipitation, its effect on tracer concentrations at low-level measurement sites on the northern site is not clearly detectable as concentrations thinned out continuously and showers occurred only local. Humidity at Jungfraujoch increased constantly caused by engulfment of mountain-top clouds. It is likely that the decrease of SO_2 is connected with the increase in humidity. PM10 stayed nearly constant at the same time. Other tracers remained in the range of background concentration and cannot be allocated to the VA layer.

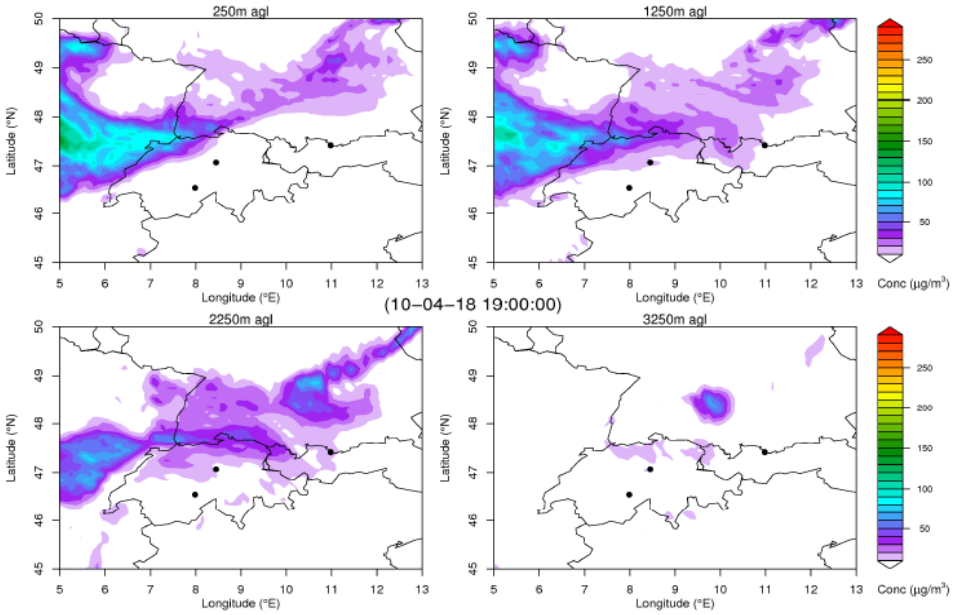

Figure 15: FLEXPART model of EMPA (source: Hüglin et al., 2010) demonstrates the heterogeneous dispersion of ash particles at several altitude levels above the modeled topography for 18 April at 20 LT.

To a large part, wind direction and speed above and downwind of the erupting volcano determined the dispersal pattern of volcanic ash in the atmosphere by enhanced entrainment of air, horizontal momentum and plume bending [Bursik, 2001]. According to Petersen [2010], it is likely that the strong winds above 3km altitude (>18ms^{-1}) over Iceland during 15 and 16 April kept the plume height lower than it would have been the case with lighter winds. Both direction and speed typically varies with increasing altitude above the ground and distance from a volcano. Significant changes in wind direction and speed can occur during a single long eruption and results in a complex and changing ash-dispersal pattern, especially in the presence of cyclonic systems. In terms of prolonged series of eruptions that last days to weeks, changing wind patterns typically blow ash in widely different directions [USGS, 2011]. In the volcanic ash dispersion models, these advection and diffusion processes were visible during the eruptions of Eyjafjallajökull who were governed by differing eruption strengths, wind patterns and eruption heights.

4.4.2 Early May event

- **Meteorological situation**

  Europe: For the early May phase the situation varied due to an additional upper low pressure zone at 500mbar geopotential height with its core above Southern Great Britain. This synoptic system steered the upperlevel Icelandic airmasses towards the westernmost regions of Europe.

  Switzerland: During 9 May a frontal zone crossed Switzerland and increased the degree of cloudiness (mostly broken to overcast). Payerne sounding of 12 UTC revealed a high relative humditiy throughout all layers and radar signals showed widespread little to moderate precipitation (all selected NABEL sites between 3-27 mm per day). Windspeeds picked up to 40 knots (kts) on the upper levels and originated from southwest (weak Südfoehn over the Alps).

- **Comparison with measurements**

  Time series of Jungfraujoch and Basel show only weak simultaneous alterations of PM10 and SO_2 on 9 May. Other measurement sites did not record any significant simultaneous increases of both tracers. Concentrations were generally very low. Regarding other tracers, just a 10% decrease of O_3 at Jungfraujoch (morning of 9 May) was remarkable. The Metair profile approves the generally low concentrations measured at NABEL sites. However, a faint VA layer above 4000m AMSL can be noticed.

  During this phase, airmasses from Iceland were transported around a low pressure system over Portugal eastwards across the Mediterranean Sea. Ash layers are therefore driven around this strong low which caused a large-scale wash out. Therefore concentrations (except on altitudes higher than approx. 5000m AMSL) should be lowered, but also due to the generally longer distance around this cyclone. These effects were clearly visible in both data sets. The mostly very humid airmasses and widespread precipitation across Switzerland in combination with southwesterly winds led to a different meteorological situation compared to Mid April.

4.4.3 Mid May event

- **Meteorological situation**

  Europe: An anticylone over the Atlantic and lows over Portugal and Eastern Europe marked the synoptic situation (pattern). Cool air with moderate humidity reached the Alps from Northwest.

  Switzerland: On 18 May, humidity was much lower in certain layers and showers occurred only at some locations on the northern side of the Alps due to orographic induced precipitation (NABEL sites below 3mm/day, see appendix B). Winds from a northwesterly

direction were weak on the surface but stronger with increasing altitudes. The pressure distribution was shallow enabling the lift of airmasses (table 5).

Table 5: Meteorology in Switzerland during measurement flight days including cloudiness (Metair pictures, archive of meteo.sf.tv, wetter3.de) and precipitation (radar and satellite images (source: Eumetsat, provided by Meteotest), NABEL data); winds in Payerne at different levels (according to 12 UTC Payerne soundings with upper wind level (above 2000m AMSL) and lower level (below 2000m AMSL)); winds and humidity at Jungfraujoch ([Bukowiecki et al., 2010], archive of meteo.sf.tv); inversion altitude (Payerne 12 UTC soundings); pressure gradient (wetter3.de) and CAPE (convective available potential energy; sounding Payerne 12 UTC).

	Cloudiness	**Areas with precipitation**	**Midlands: Wind above 2000m AMSL; below 2000m AMSL**	**Jungfraujoch: Wind; Humidity at 3500 AMSL**	**Inversion altitude; Pressure gradient; CAPE (measured at Payerne)**
17.4.2010	fair but hazy weather in the north; cloudy in the south	some showers in Ticino	NE, 20-40kts; NE, < 15kts	SE, <20kts; dry conditions	weak inversion: 1200m AMSL; subsidence; no CAPE
18.4.2010	mostly hazy, fair weather; cloudy in the Alps/ South	showers in Ticino, few showers along Alps and Prealps	W/N, < 20kts; VAR, <10kts	NW, < 20kts; very humid (cloudy)	isotherm: 2000m AMSL; weak subsidence; moderate CAPE
19.4.2010	improving fair weather, cumulus above Alps	some rain along Jura, Lowlands and Prealps	W-N, < 15kts; SW, < 10kts	NW, < 20kts; very humid (cloudy)	weak inversion: 2500m AMSL; subsidence; low CAPE
9.5.2010	several cloud layers; scattered to overcast	widespread precipitation	SW, < 40kts; SW, < 2kts	SW, < 30kts; mostly humid	no inversion; lifting airmasses; moderate CAPE
18.5.2010	partly cloudy, overcast along Northern Alps, Nordföhn	some showers mainly along the Northern Alps	NW, >30kts; NW, <5kts	NW, < 30kts; very humid	inversion: 3000 AMSL; lifting airmasses; low CAPE

- **Comparison with measurements**

  In contrast to the insignificant early May phase, measurements on 18 May clearly depicted VA layers. Jungfraujoch reached the highest PM10 and SO_2 concentrations of the whole eruption episode. Also Lugano had a strong simultaneous increase of both tracers. Basel, Zürich, Härkingen and Rigi show certain increases, but cannot be assigned to the VA layer with certainty. Other tracers remained on the background noise level. Only the simultaneous O_3 decrease at most low-level sites (6 LT) was unusual. The Metair profile indicates interesting processes on this day as not only particle concentrations were strongly increased, but also CO_2 and CO. The strong drop in O_3 concentrations lies far outside of the background noise and definitely belongs to the gas phase of the VA layer.

  The synoptic situation in May led to shorter air parcel trajectories compared to 9 May, thus airmasses approached Switzerland more directly implying higher concentrations. The prevailing Nordfoehn condition with winds from northwesterly directions led to high humidity along the northern side of the Alps, but also steered downslope winds into the valleys of Ticino. Strong increase in PM10 concentrations corresponds to this situation at Jungfraujoch and Lugano by the transport of free tropospheric VA airmasses towards the surface.

  Compared to the dryer April phase, lower concentrations of PM10, CO_2 and other tracers were measured in mid May within the troposphere. One possible reason for the reducction in PM10 is the enhanced wash out process. Other tracers however are not scavenged easily and are most likely diluted by the mixing of the PBL with the FT. Stratification seems therefore to be an important factor for concentrations within the PBL. However, as these parameters within the PBL are mostly man-made, the stratification effect is only relevant if low-level volcanic air masses advect directly into the PBL (e.g. Basel in mid April).

4.5 Ageing processes

Thesis: Both phases within the VA plume are exposed to the same meteorological conditions. Thus,the dilution rate of the aerosol phase corresponds to the decrease of the gas phase concentration in the same time span. In rainy conditions, it is expected that the particles are washed out faster, whereas the gas phase phase remains nearly constant.

The most appropriate tracers for each phase were already defined in chapter 4.3 (SO_2 for the gas phase and PM10 for the particle phase, respectively). Airborne measurements would show clearly the maximum peaks of PM10, but due to lack of SO_2 data and missing continuous measurements above a defined location (heterogeneous distribution of VA within Switzerland might distort Metair data), ground based data on Jungfraujoch were used for the analysis of the dilution rate for both phases.

For the April event, a 33% decrease within 5 hours was measured for SO_2, whereas PM10 concentrations declined by 28% within the same time span. Thus, both phases decline by a factor 1.5 per day, which corresponds to a dilution factor of 2 for both phases measured in Germany [Schumann et al., 2011]. This value seems therefore to be reasonable meaning that both phases dilute by the same factor under fair weather conditions (present during April phase). For wet conditions, the dilution rate seems to be slightly higher. A sample on 18 May between 20 and 23LT shows a dilution rate of 37% for PM10 (54.4µm/m^3 to 20.2µm/m^3) and decline in SO_2 concentration of 38% (12.3ppb to 4.7ppb), both phases corresponding to a dilution factor 3 per day.

Although the decline rate for both phases appear to be almost identical , the SO_2/PM10 ratio differs strongly, depending on the weather conditions (table 6). Jungfraujoch presents a weaker correlation of SO_2/PM10 for the April phase and a very strong relation for 18 May. Rigi and also measurement sites within the PBL show higher correlations for the May episode than for April. The correlation values of SO_2/PM10 for the 15 days before the first arrival of a VA plume are diverse, depending mostly on anthropogenic sources. Still the difference between non-volcanic and volcanic events is significant and indicate VA airmasses.

Table 6: Correlation values and slopes of SO_2 [ppb] /PM10 [µm/m^3] for non-volcanic phases (1.-15.4.2010), and the two volcanic events in April (17.-19.4.2010 and May (18.5.2010)), data: NABEL (BAFU and EMPA).

	Lugano		Zürich		Basel		Härkingen		Rigi		Jungfraujoch	
	corr.	slope	corr.	slope	corr.	slope	corr.	slope	corr.	slope	corr.	slope
Non-volcanic phase	0.20	2.4	0.23	4.4	0.04	0.6	0.46	20.4	0.56	54.6	0.24	31.7
Volcanic event April	0.31	2.0	0.60	5.5	0.72	7.3	0.81	14.5	0.43	3.0	0.73	11.8
Volcanic event May	0.94	7.7	0.84	10.7	0.86	18.7	0.89	20.4	0.85	10.3	0.97	4.7

The SO_2/PM10 slopes of table 6 are presented in the following graph (figure 16). Obviously, Rigi and Jungfraujoch shows the steepest slopes in non-VA phases, probably because they measure mostly background concentration of the free troposphere, compared to the flat gradients of all the other sites measuring the PBL. However, a tendency between April and May slopes is visible for all ground based sites. In general, May slopes are steeper indicating a higher SO_2- or lower PM10-value than in April. For each site, the gradient is factor 1.5 to 4 steeper compared to their April gradient.

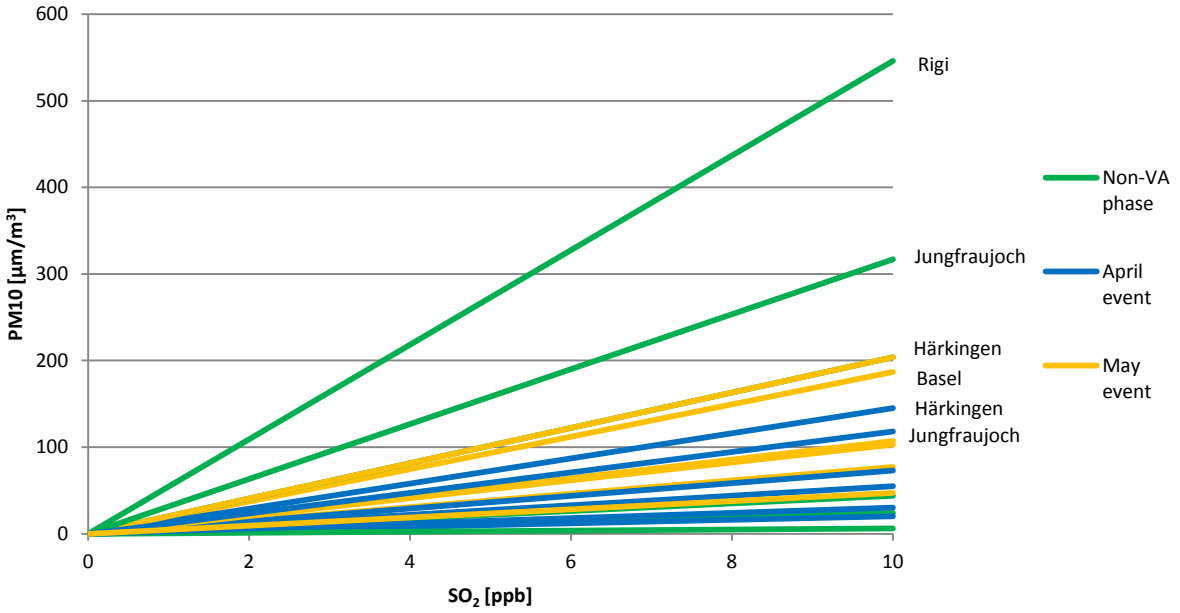

Figure 16: SO_2/PM10 slopes of Lugano, Zürich, Basel, Härkingen, Rigi und Jungfraujoch during non- volcanic phases and two volcanic events (data: NABEL (BAFU and EMPA)).

One reason of the difference in slope of the SO_2/PM10 ratio is the variable deposition of aerosols. In fair weather, the dilution of aerosol concentration is largely dominated by wind conditions and dry deposition. The settling velocity is defined by Stoke's law and depends on density, gravity acceleration, the radius of the particle and on the dynamic viscosity of the fluid [Hinds, 1982]. Because the settling velocity is proportional to the square of the particle size, a 100µm particle settles 10^6 times faster, and would settle a distance of one meter in only three seconds (http://www.cee.mtu.edu). Previous analysis of Mount St. Helens shows that particles with a mean diameter of 100µm and larger settled within 200km downwind the source [USGS, 2011]. These settling distances are also dependent from the windspeed. In the case of the Eyjafjallajökull plume, particle sizes from a sample at Mýrdalssandur (50km from Eyjafjallajökull) were distributed as follows: 24% under 10µm diameter; 33% between 10 and 50µm; 20% between 50 and 146µm as well as 23% between 146 and 294µm [Smithonian Institution, 2010]. According to combined OPC and SMPS measurements, the largest particles arriving in Switzerland after approximately 2500km were

between 10 and 20µm in diameter. Thus, the number of larger particles reaching Switzerland in dry conditions is a function of distance to the source, whereas in rainy weather, more particles are removed by wet deposition. Paradoxically, figure 12 shows higher particle numbers in the coarse mode for wet May although the travel time for the airmasses was the same in April and May (2.5 days according to HYSPLIT backward trajectory models). This is most likely caused by a change in eruption characteristics (Heue et al., 2011). However, also the heterogeneous dispersion of the VA cloud within Switzerland probably falsified the PM10 factor.

Another reason for the difference in slope gradient is the processing of SO_2. Within the troposphere, SO_2 is mainly controlled by the humidity of ambient air. As small sulfuric acid particles are more efficiently captured by cloud droplets, they could subsequently be removed from the atmosphere by wet deposition more efficiently [Flentje et al., 2010]. Examining the April sequence, SO_2 starts to drop as soon as the measurement site at Jungfraujoch is engulfed by clouds (locally enhanced relative humidity of > 95% on 18 and 19 April). It is likely that, in these wet PBL-processed airmasses, SO_2 to sulfate conversion was fully completed before the arrival at the Jungfraujoch; either in local clouds or at an earlier stage [Bukowiecki et al., 2010]. On the other hand, the change in eruption composition (substancially higher amount of SO_2 emitted in May than April, [Thomas and Prata, 2011]) might have also led to a higher SO_2/PM10 ratio. A third option is the reduction of SO_2 by hydroxyl radical, which are dominant in fair weather. As the April phase was more stable and received more radiation, enhanced hydroxl radical concentrations might have also led to a smaller SO_2/PM10 ratio at all measurement sites. However, Anderson et al. [1989] learned that hydroxl radical reactions with SO_2 do not act as a radical sink under atmospheric conditions. Therefore, the influence of humidity seem to be most important for SO_2 conversion.

4.6 Chemical processes

Previous large volcanic eruptions showed a decrease in O_3 mostly due to reactive processes with SO_2. Emitted SO_2 of Eyjafjalla is therefore expected to lead to a depletion in O_3 in the respective volcanic air layer.

O_3 concentration depletion in VA layers are only considerably visible in the Metair profile of 18 May (figure 8). 17 April profile (figure 7) also shows a clear depletion, but with a shift upwards in altitude (approximately 100 meters above the layer of particles). As O_3 is a very reactive oxidizing gas and reacts on nearly all types of surfaces, its vertical distribution should be visible quickly. The reason for the phase shift on 17 April might be the depletion of O_3 reacting with surfaces of particles, who have afterwards subsidized faster than the gas phase. In contrast to the Metair profiles, almost no significant decreases in O_3 are present at NABEL sites. In terms of low-level sites, the long-lasting subsidizing and dilution processes into the PBL make it nearly impossible to identify any decreases. The only high-alpine measurement site at Jungfraujoch might be appropriate to detect a significant decrease in O_3. However, this was not the case during Eyjafjallajökull eruptions.

Another possible mechanism would the reaction with BrO. However, according to Gerlach [2004] this gas must be present in the dimension of [ppb], but Eyjafjallajökull emitted only amounts in a mixing ratio dimension of [ppt]. Therefore, BrO cannot be responsible for any decreases in vertical O_3 depletion.

Regarding reactions with SO_2, it seems unlikely that they influence the O_3 concentration, as the emitted amount with 3000-6500 tons per day [Smithonian Institution, 2010; Allard et al., 2011] was very low compared to other large eruptions (Pinatubo: 22 Mio. tons). On the other hand, Thomas et al. [2011] stated that emitted SO_2 amount in May were exeeded the April quantity by far. It is plausible that surface reactions caused the depletion of O_3 concentrations ([Köhler et al., 2010]), probably together with an relatively low, but still increased SO_2 concentration.

5 Conclusion and Outlook

5.1 Conclusion

The meteorological situation certainly affects the characteristics of gas and aerosol phases. Precipitation leads to a increased wash out of larger particles by wet deposition. Winds define the plume height (decreasing when increasing winds with altitude), the distibution pattern of the VA layer and the duration for aerosols to settle (the weaker the wind, the slower airmasses drift, whereby larger particles have more time to settle). In terms of atmospheric stratification, stable conditions lead to an increase in concentrations within the PBL compared to instable convective stratification. However, concentration fluctuations within the PBL are mostly man-made, as VA layers already diluted strongly when down-mixing with PBL occurs.

Regarding the ageing processes of gas (tracer: SO_2) and particle phase (tracer: PM10), the dilution rate is almost identical. In moist weather however, the dilution factor per day is approximatley double the dilution factor for fair weather conditions (1.5). Whereas the reduction of particles are mainly determined by gravitational sedimentation and wet deposition (precipitation scavenging and in-cloud scavenging particularly in May), the main mechanisms controlling SO_2 are reactions with OH radicals and wet deposition. Especially humid conditions (e.g. cloud-engulfment situation at Jungfraujoch in April) led to a conversion of SO_2 into H_2SO_4.

In terms of O_3 reduction, SO_2 concentrations are relatively low in number concentration to influence the O_3 vertical profile significantly. However, as the chemical composition of the VA plume changed in May, it its likely that SO_2 increased and thus caused a visible footprint in the Metair profile of 18 May. Also surface reactions with emitted particles contributed to the O_3 depletion.

Due to methodical and technical uncertainties (see appendix), the outcomes of the thesis may have been influenced to a certain degree. Additionally, the analysis process demonstrated, that in terms of *in-situ* ground measurements, only Jungfraujoch is appropriate due to its remote, mostly non-PBL-influenced location, especially throughout the night. Regarding tracers, results showed that only PM10 and SO_2 are appropriate tracers to indentify VA layers. Although other tracers were emitted in large amounts or possess metastable properties, they were not clearly detectable anymore in Switzerland, as the atmospheric diffusion and advection as well as chemical processes along the path diluted the initial concentrations into unrecognizable background noise.

5.2 Outlook

Patrick Allard of Paris Institute for Global Physics estimates the CO_2 emissions of Eyjafjallajökull amount to 150‘000-300‘000 tons per day. This would result in a netto GHG effect equal nil due to the emission compensation by grounded airplanes. Although the eruption in 2010 did not cause climatic fluctuations (not enough material was injected into the stratosphere), other large volcanoes can have and already had far-reaching short- and long-term impacts on human health, environment, economy and climate. Physical and chemical processes of airmasses containing volcanic emissions are complex but important to conceive regarding the ongoing progress of model development. The more knowledge we gain of small-scale short-term processes, the more precise we can estimate climate impacts leading to an overall improvement of long-term models. Especially concerning *in-situ* measurements, the case of Eyjafjallajökull was a unique opportunity for atmospheric research and enabled a detailed analysis with high temporal and spatial resolution. This large amount of data served, among other studies, as a validation of dispersion models with the result of good agreement relating to the extension of spatial distribution. However, particle mass concentrations coincided only moderately with the measured *in-situ* data. In order to improve climate models and to accomplish appropriate forecasting air space closures in the future, characteristics of volcanic ash plumes need to be better unterstood. Therefore, further research in transport and ageing processes of volcanic ash is essential.

Appendix

➢ Uncertainties

Technical and methodical uncertainties

Metair data were strongly influenced by transport losses in the sampling line. For the Grimm 1.108, transport losses were estimated to be 15% for aerodynamic diameters of 3 µm; and larger than 60% for > 6µm; MetOne OPC > 60% sampling loss for aerosols larger than 0.6 µm. Also deviations of ideally isokinetic sampling conditions depending on true air speed, inclination angle, volumetric sample flow rate and sampling efficiency influenced the measurements. For larger aerosols the influence on the sampling efficiencies becomes even more pronounced. Both Grimm and MetOne data were corrected; additionally April MetOne measurements were calibrated with the more precise Grimm data of their common employment in May. However, these corrections were only applied to particle number concentrations and not to the gas phase measured by Metair. Therefore, gas phase values can only be considered in a qualitative way [Bukowiecki et al., 2010]. Inappropriate values (NO_2) were neclected for the analysis.

Metair humidity measurements are only valid for a range between 20-95% relative humidity. The values were generally used for a qualitative assessment and were also intercompared with other data. Those other meteorological parameters with varying temporal and spatial resolutions were analysed retrospectively. Because the aerosol distribution was very heterogeneously distributed on the horizontal axis, a more detailed interpretation in terms of wind transport or wash out processes would have been unreliable and was therefore neglected.

NABEL O_3 data contain measurement uncertainties which are determined by error propagation of the influence factors' standard errors. For certain mixing ratios, extended measurement uncertainties are determined to define 95% confidence intervals. For a measured value of 20ppb, the true value lies within 19.85 and 20.85ppb with 95% certainty. Generally, uncertainties become smaller with increasing mixing ratios. In April, measurement values ranged within 20 and 120 ppb considering all NABEL measurement sites, impyling uncertainties between 2% and 10%. Uncertainties of other parameters can be looked up in EMPA [2010].

Incomplete capture of bimodal aerosol distribution

Besides the technical uncertainties, also differences caused by aerosol properties need to be regarded. The particle shape has a strong impact on the refractive index. Grimm measurements are only appropriate when particles are spherical; else a shift in size distribution cannot be excluded. A correction therefore was performed, but some uncertainties remain [Bukowiecki et al. 2010]. Also the relationship between aerosols number concentration and aerosol volume concentration is

important regarding the outcomes of the thesis. Whereas a few large particles strongly increase the respective volume concentration of this certain particle diameter, they are rarely visible in number concentration plots due to its strong decrease with increasing particle size [Schumann et al., 2010]. Therefore, the second peak of the bimodal aerosol distribution of volume concentration (1. peak around 0.3µm; 2. peak around 3µm) has not been captured entirely by MetOne number concentrations plots (statement of Bruno Neininger).

Influence of planetary boundary layer on measurements

Whereas increasing PM10 and SO_2 concentrations measured by Jungfraujoch and Metair generally clearly depicts the presence of a volcanic ash layer, these parameters blur inside the PBL by the masking of anthropogenic emissions. The influence of PBL mostly masks the VA signal for the five selected lowlevel sites (Basel, Bern, Zürich, Härkingen, Lugano) and solely very strong increases of certain parameters are visible, most likely through advectional processes (e.g. Basel or Föhn in Lugano). Also when considering other lowland sites (e.g. Payerne, Tänikon), results do not alter significantly. Elevated sites need to be preferred, although Rigi on 1000m AMSL did not deliver many significant data. Therefore, Jungfraujoch in the FT is most appropriate for ground based *in-situ* measurements of VA plumes.

Lagrangian models

Model outputs of the VA plume were appropriate in spatial extent of the plume, but not very precise with particle concentrations [Neininger, 2010; Hüglin et al, 2010]. The main reasons for these errors are the lack of knowledge in terms of source strength (ash mass flux, [Schumann et al., 2011]) as well as particle size distribution (which influences the diffusion pattern due to gravitational settling). However, the inclusion of satellite-retrieved data to model time-height development of the ash plume led to a significantly improved result in the case of Eyjafjallajökull [Stohl et al., 2011].

➢ Conversion of µg/m³ into ppb (or mg/m³ into ppm)

$$c_i[\mu g/m^3](p,T) = c_i\,[ppb] \cdot \frac{p \cdot M^i}{T \cdot R}$$

c_i [µg/m³]	mass concentration of the gas i in µg/m³
c_i [ppb]	substance amount fraction of the gas i in ppb
p	atmospheric pressure in Pascal (1mbar = 100 Pasccal)
T	temperature in Kelvin
M_i	molar mass of the gas i in kg/mol
R	molar gas constant: 8.314 J/mol K

NABEL sites below 1500m AMSL:
1013.25mbar and 293.15K

Jungfraujoch measurement site:
653mbar and 265.15K

For the specific conversion factors of the gas concentrations, consult EMPA [2010] on page 184.

➢ Appendix A - Figures

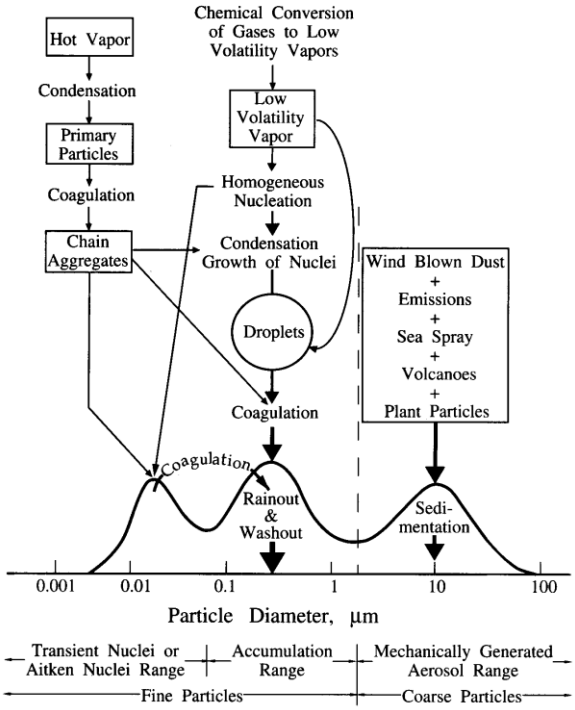

A1: Different particle modes including the typical diameters and processes of nucleation (or Aitken), accumulation and coarse mode. Especially the accumulation and coarse mode are enhanced in the case of Eyjafjallajökull in Switzerland. The conversion of sulfuric acid into sulfate contributed to the intermediate mode between approximately 0.1µm and 1µm. The largest particle mode is increased through enhanced fine dust and soot concentration. However, particles larger than roughly 10µm occurred scarcer due to sedimentation and wash out processes (source: http://cloudbase.phy.umist.ac.uk).

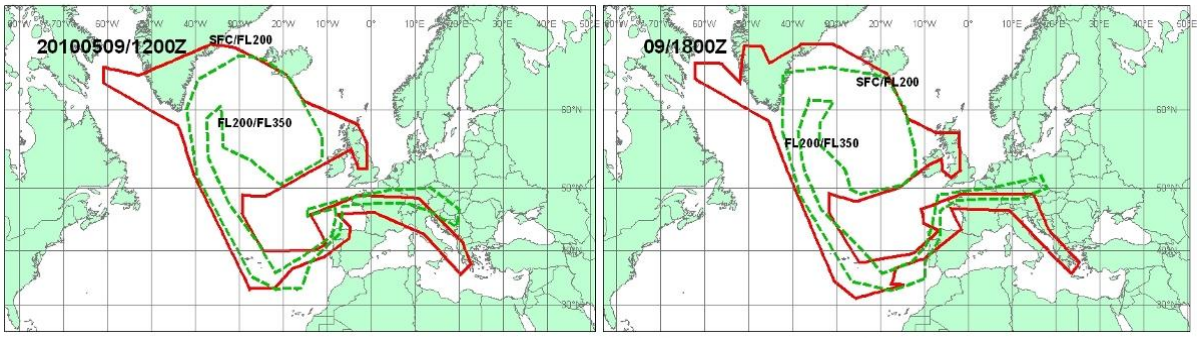

A2: Compilation graphic of daily Volcanic Ash Advisories showing the assessed or interfered extent of ash plumes at 12 and 18 UTC of 9 May 2010. "SFC/FL200" denotes the green area covered by the ash advisories at altitudes from the surface to flight level 200 (20'000ft); "FL200/FL350" the red area for altitudes between 20'000ft and 350'000ft. The detour of the VA plume around a cyclonic system is well visible (URL: http://www.meteoradar.ch, access: 2.5.2011).

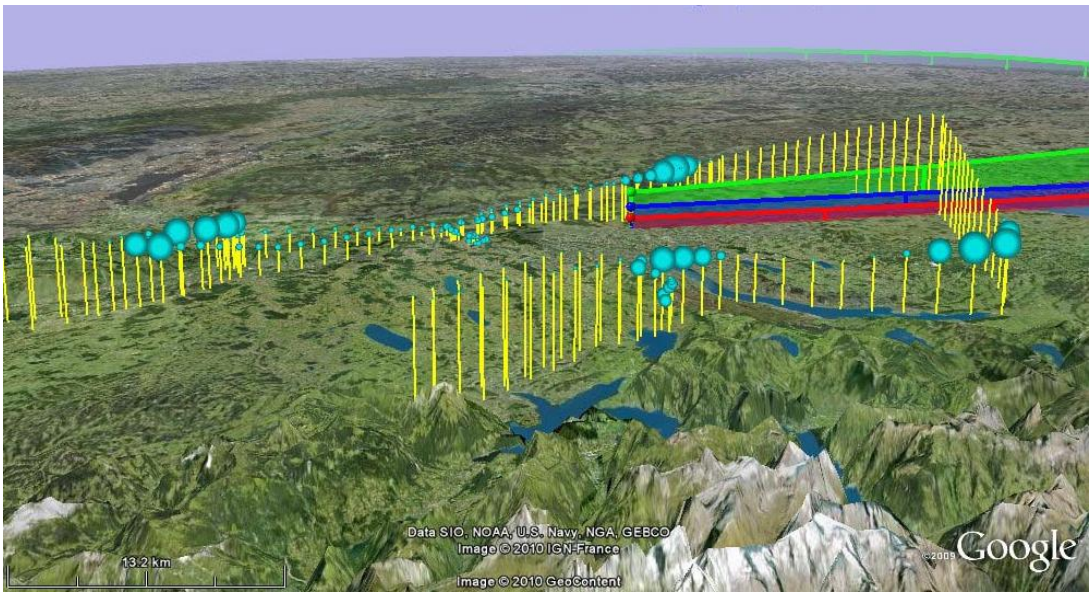

A3: Metair flight tracks of 17 April between 12 and 17 LT with a first ascent towards northeast. Yellow bars indicate flight altitudes above ground; blue dots on top are proportional to particle concentrations larger than 0.5µm. The red, blue and green backward trajectories (HYSPLIT) from the east illustrate advecting airmasses at different levels. Especially the green air layer stems from the area south of Iceland and indicates therefore enhanced particle concentration which is also apparent regarding enlarged blue dots (source: Neininger, 2010).

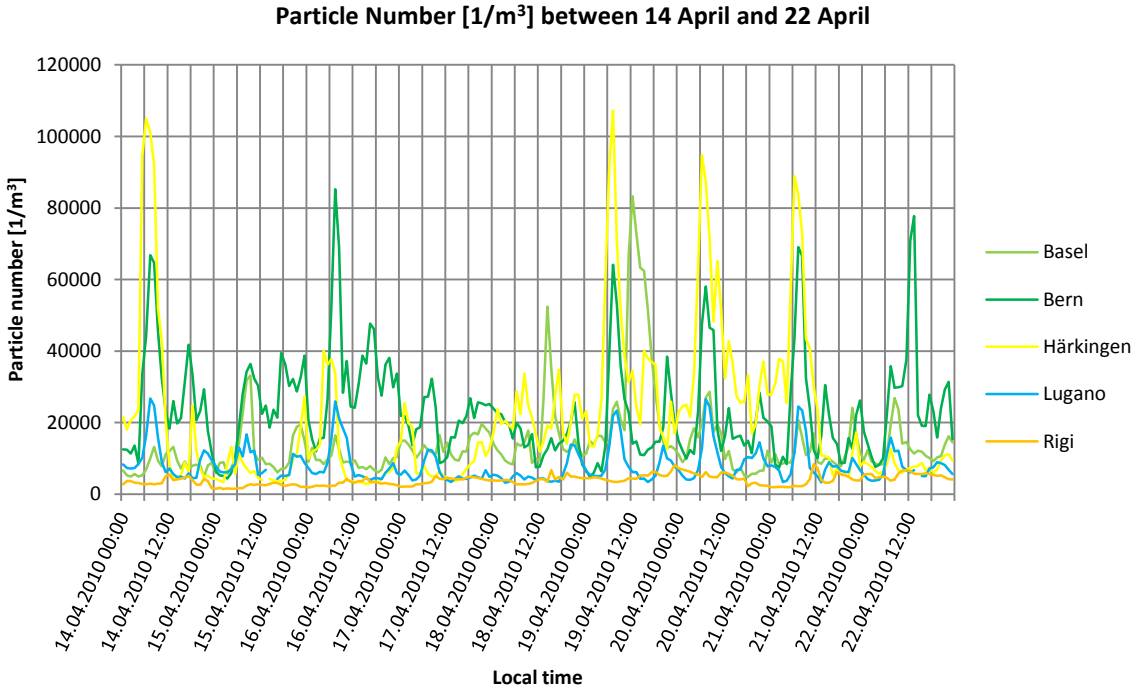

A4: Particle number of some NABEL measurement sites during April phase. Except Basel on 18 and 19 April, all other sites show values inside the background concentration levels (data: NABEL (BAFU and EMPA)).

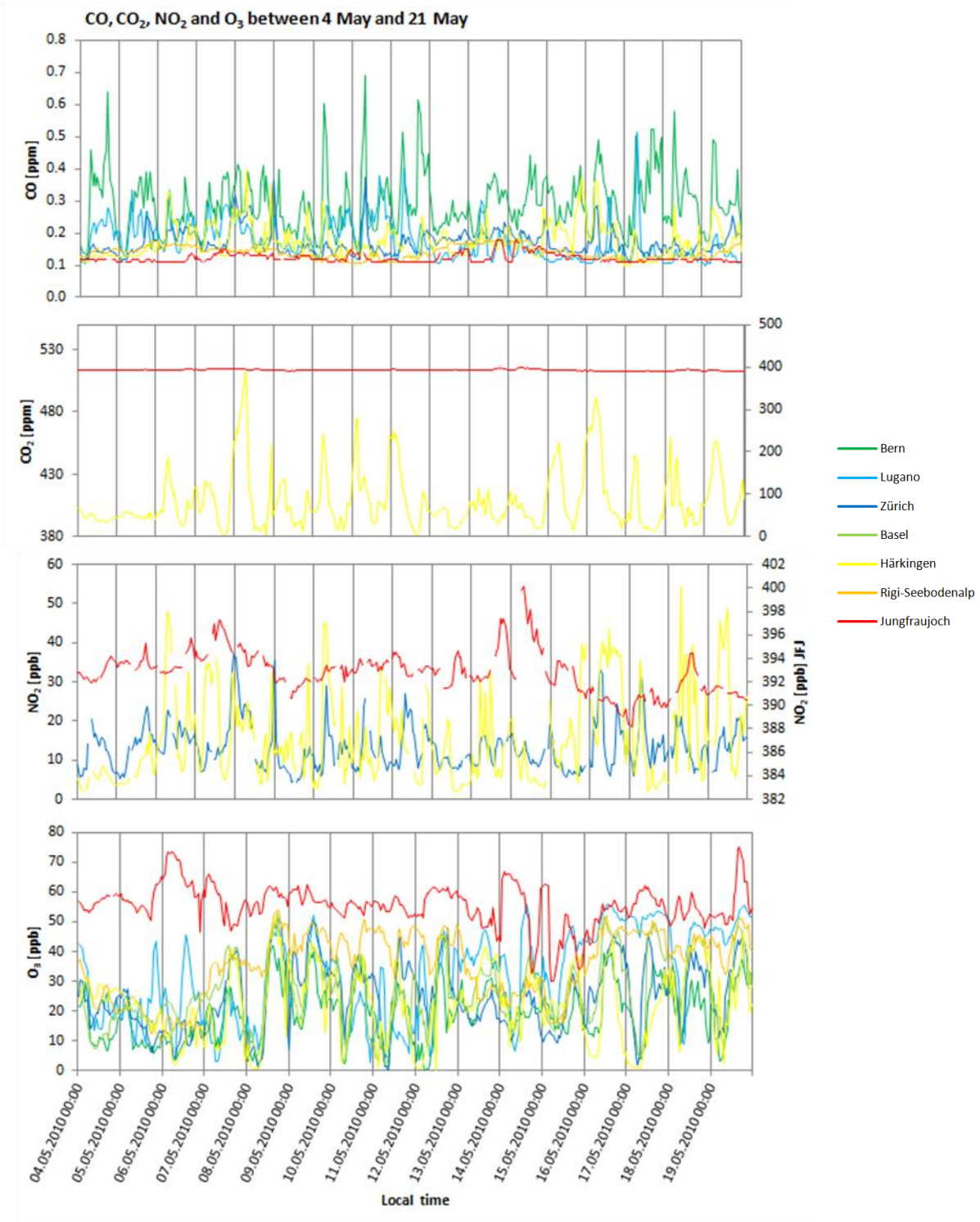

A5: NABEL Measurements of CO, CO_2, O_3 and NO_2 from 4 May 00 LT to 20 May 00 LT (data: NABEL (BAFU and EMPA)).

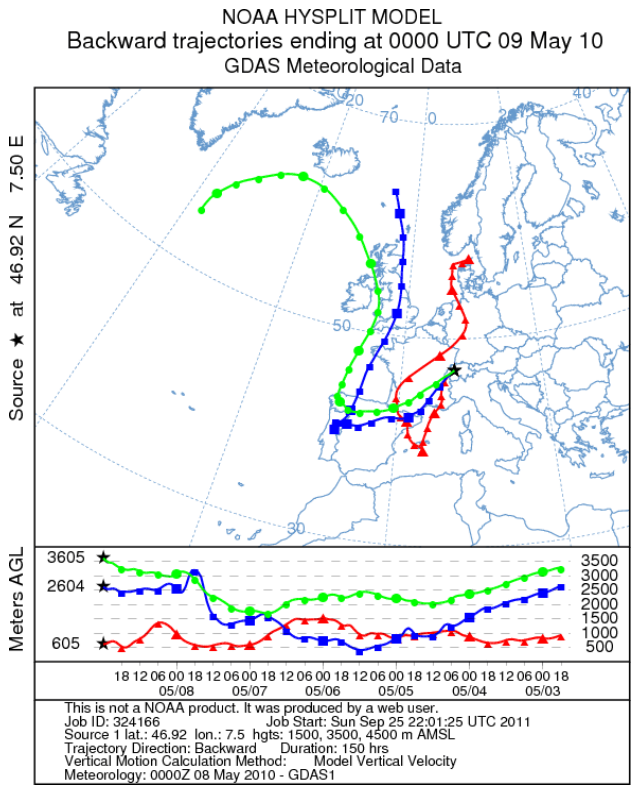

A6: Interactive Output of NOAA HYSPLIT model for 150h backward trajectories of 9 May OO UTC with the source Bern-Belp and GDAS meteorological input data. Heights of three defined trajectory-ending levels over Bern were set at 1500m, 3000m and 4500m AMSL. Air parcels at higher altitudes (green) originated from Iceland and contained volcanic ash. The detour around a low pressure system over Western Europe caused enhanced wash out and settlement due to a longer trajectory compared to April trajectories (source: ready.arl.noaa.gov, access: 25 Sept 2011).

➢ Appendix B - Tables

	Bern	Lugano	Zürich	Basel	Härkingen	Rigi
17.04.2010	-	3.4	-	-	-	-
18.04.2010	-	1.1	-	-	-	2.2
19.04.2010	0.1	-	0.2	-	-	0.2
09.05.2010	8.3	27.1	3	15	9.7	3
18.05.2010	0.2	-	0.7	-	0.5	2.8

B1: Daily total precipitation on research flight days in April and May 2010 (sum of hourly mean precipitation, data: NABEL (BAFU and EMPA)).

		Individual Gases					
Data	**Altitude**	**CO**	**CO_2**	**SO_2**	**O_3**	**NO_2**	**H_2O**
NABEL/EMPA/PSI	**[m] AMSL**	**h mean**	**h mean**	**h mean**	**h mean**	**h mean**	**[mm] h mean**
Basel	317	-	-	X	X	-	X
Bern	536	X	-	-	X	-	X
Härkingen	431	X	X	X	X	X	X
Jungfraujoch	3578	X	X	X	X	X	-
Lugano	281	X	-	X	X	-	X
Rigi-Seebodenalp	1031	X	-	X	X	-	X
Zürich	410	X	-	X	X	X	X
Measurement method		NDIR-absorbtion	Infrared spectrom.	U-fluorescence	UV-absorbtion	chemilumenescence	water gauge
Measurement systems		Horiba AMPA360	LICOR Li-7000	Thermo 43C TL	Thermo 49c	Horiba ABNA360	pluviometer
		Horiba AMPA370	Picarro G301	Thermo 43i TLE	Thermo 49i	Thermo 42i, etc.	
Source		NABEL	NABEL	NABEL	NABEL	NABEL	NABEL
METAIR		**1Hz**	**1Hz**		**1Hz**	**1Hz**	**rel. Humidity**
17/ 18/ 19 April	max 6000	X / - / X	X / X / X	-	X / - / X	X / - / X	X / - / X
9/18 May	max 4800	X / X	X / X	-	- / X	X / X	X / X
Measurement method		Resonance-fluorescence	Differential infrared gas analyser	-	UV-absorption	Luminol-detector	Differential infrared gas analyser
Measurement system		Aerolaser AL-5003	LICOR 6262/ 7500	-	PSI/ Monitor Labs	METAIR-NOxTOY	LICOR 6262/ 7500

Data	**Altitude**	**Particles**						
NABEL/EMPA/PSI	**[m] AMSL**	**PM1 daily mean**	**PM10 h mean**	**Part. # h mean**	**>0.3 µm**	**>0.5 µm**	**0.3 - 20 µm**	**10-487 nm**
Basel	317	X	X	X	-	-		
Bern	536	X	X	X	-	-		
Härkingen	431	X	X	X	-	-		
Jungfraujoch	3578	-	X	-	-	-	X	X
Lugano	281	X	X	X	-	-	-	-
Rigi-Seebodenalp	1031	X	X	X	-	-	-	-
Zürich	410	-	X	-	-	-	-	
Measurement method		comb. method	comb. method	CPC			OPC	Spectrometer
Measurement systems		HIVOL&TEOM	HIVOL&TEOM	TSI 3775A			GRIMM	TSI SMPS
				TSI 3022A				
Source		EMPA	EMPA	EMPA			PSI	PSI
METAIR								
17/ 18/ 19 April	max 6000	-	-	-	X / X / X	X / X / X	-	-
9/18 May	max 4800	-	-	-	X / X	X / X	X / X	-
Measurement method					OPC	OPC	OPC	
Measurement system					Met One	Met One	GRIMM 15 bins	

B2: These tables give an overview of analysed particle and gas measurement methods and systems for this master thesis. More data would be available but were not regarded or applied. This list is therefore not intended to be exhaustive (data: Metair and [EMPA, 2010]).

List of Tables

List of Figures

Bibliography

ALLARD, P., M. Burton, N. Oskarsson, A. Michel, and M. Polacci: Magmatic gas composition and fluxes during the 2010 Eyjafjallajökull explosive eruption: implications for degassing magma volumes and volatile sources, Geophysical Research Abstract, Vol 13, 2011.

ANDERSEN, U.J., E. Kaas, and P. Alpert: Using analysis increments to estimate atmospheric heating rates following volanic eruptions, Geophys. Res. Lett., 28, 991-994, 2001.

ANDERSON, L.G.; P.M. Gates, C.R. Nold: Mechanism of atmospheric oxidation of sulfur dioxide by hydroxyl radicals, Biogenic Sulfur in the Environment, 437-449, 1989.

BLUNDEN, J., D.S. Arndt, M. O.Baringer: State of the Climate in 2010, Bull. Amer. Meteor. Soc., 92, 6, 1-266, 2011.

BRÖNNIMANN, S.: Large-scale climate variability, lecture notes, 2010.

BUKOWIECKI, N., P. Zieger, E. Weingartner, Z. Jurányi, M. Gysel, B. Neininger, B. Schneider, C. Hueglin, A. Ulrich, A. Wichser, S. Henne, D. Brunner, R. Kaegi, M. Schwikowski, L. Tobler, F.G. Wienhold, I. Engel, B. Buchmann, T. Peter and U. Baltensperger: Ground-based and airborne in-situ measurements of the Eyjafjallajökull volcanic aerosol plume in Switzerland in spring 2010, Atmos. Chem. Phys. Discuss., 11, 12949-13002, 2010.

BURSIK, M.: Effect of wind on the rise height of volcanic plumes, Geophys. Res. Lett. 18, 3621–3624, 2001.

CHIN, M., and D. J. Jacob, Anthropogenic and natural contributions to tropospheric sulfate: A global model analysis, J. Geophys. Res., 101, 18, 691–18, 1996.

COLLAUD COEN, M., Weingartner, E., Schaub, D., Hueglin, C., Corrigan, C., Henning, S., Schwikowski, M., and Baltensperger, U.: Saharan dust events at the Jungfraujoch: detection by wavelength dependence of the single scattering albedo and first climatology analysis, Atmos. Chem. Phys., 4, 2465–2480, 2004.

DEGRUYTER, W.: Exploring the potential of digital image analysis of SEM and Micro-CT images of accretionary lapilli, master thesis, University of Gent, 2006.

DRAXLER, R., and G. Rolph: HYSPLIT4 model (Hybrid Single-Particle Lagrangian Integrated Trajectory) model, URL: http://www.arl.noaa.gov/ready/HYSPLIT4.html, Access: 7. Aug 2011, NOAA Air Resources Laboratory, Silver Spring, Maryland, 2003.

EMPA, BAFU: Technischer Bericht zum Nationalen Beobachtungsnetz für Luftfremdstoffe (NABEL) 2010, Dübendorf, 2010.

EUFAR (European facility for airborne research): URL: http://www.eufar.net/wiki/pmwiki/pmwiki.php/EufarCMS/VolcanicAshes?skin=view, Acess: 15 August 2011, 2010.

FISCHER, E.: Climate response to major volcanic eruptions, Institue for Atmospheric and Climate Science ETH Zürich, URL: www.iac.ethz.ch/people/fischeer/docs/pages_erich_fischer.pdf; Access: 17 August 2011, 2006.

FLENTJE, H., H. Claude, T. Elste, S. Gilge, U. Köhler, C. Plass-Dülmer, W. Steinbrecht, W. Thomas, A. Werner, and W. Fricke: The Eyjafjallajökull eruption in April 2010 – detection of volcanic plume using in-situ measurements, ozone sondes and lidar-ceilometer profiles, Atmos. Chem. Phys., 10, 10085–10092, 2010.

GERLACH, T. M.: Volcanic sources of tropospheric ozone-depleting trace gases, Geochem. Geophys. Geosyst., 5, Q09007, 2004.

GUDMUNDSSON, M. T.: Subglacial volcanic activity in Iceland. In: C. Caseldine, A. Russell, J. Hardardóttir and Ó. Knudsen, Iceland: Modern Processes, Past Environments, Elsevier, 127–151, 2005.

HACH: MetOne 4900 Series: Operator Manual for Remote Airborne Particle Counters, URL: http://shop.hach-lange.com; Access: 25 April 2011, Hach Ultra Analytics, 2004.

HENNE, S., M. Furger, S. Nyeki, M. Steinbacher, B. Neininger, S.F.J. de Wekker, J. Dommen, N. Spichtinger, A. Stohl, and A.S.H. Prévôt: Quantification of topographic venting of boundary layer air to the free troposphere, Atmos. Chem. Phys., 4, 497–509, 2004.

HEUE, K.-P., C.A.M. Brenninkmeijer, A.K. Baker, A. Rauthe-Schöch, D. Walter, T. Wagner, C. Hörmann, H. Sihler, B. Dix, U. Frieß, U. Platt, B.G. Martinsson, P.F.J. van Velthoven, A. Zahn, and R. Ebinghaus: SO_2 and BrO observation in the plume of the Eyjafjallajökull volcano 2010: CARIBIC and GOME-2 retrievals, Atmos. Chem. Phys., 11, 2973– 2989, 2011.

HINDS, W.C.: Aerosol technology, Properties, Behaviour and Measurement of airborne particles, John Wiley, New York, 1982.

HÜGLIN C., S. Henne, and R. Ballaman: Die Aschewolken des Eyjafjallajökull – auch im Nationalen Beobachtungsnetz für Luftfremdstoffe (NABEL) klar messbar, URL: http://www.empa.ch/plugin/template/empa/*/102775; Access: 27 June 2011; EMPA, 2010.

ISAKSEN, I.S.A., C. Granier, G. Myhre, T. Berntsen, S. Dalksoren, M. Gauss, Z. Klimont, R. Renestad, P. Bousquet, W. Collins, T. Cox, V. Eyring, D. Fowler, S. Fuzzi, P. Jockel, P. Laj, U. Lohmann, M. Maione, P. Monks, A.S.H. Prevot, F. Raes, A. Richter,B. Rognerud, M. Schulz, D. Shindell, D.S. Stevenson, T. Storelvmo, W.-C. Wang, M. van Weele, M. Wild, and D. Wuebbles: Atmospheric Composition Change: Climate-Chemistry Interactions, Atmos. Environ., 43, 5138-5192, 2009.

JURÁNYI, Z., M. Gysel, E. Weingartner, N. Bukowiecki, L. Kammermann, and U. Baltensperger: 17-month climatology of the cloud condensation nuclei number concentration at the high alpine site Jungfraujoch, J. Geophys. Res. Atmos., 12955-12960, in press, 2011.

JUSTUS-BISCHLER, E.: Charakterisierung optischer Partikelzähler für Messungen auf Verkehrs-flugzeugen, Diplomarbeit, Fachhochschule Coburg, Fachbereich Physikalische Technik, 2006.

KÖHLER U., H. Claude, and W. Steinbrecht: Ozonbulletin des DWD, Nr. 126, Mai 2010.

LAAKONSEN, A., et al., Upper tropospheric SO_2 conversion into sulfuric acid aerosols and cloud condensation nuclei, J. Geophys. Res., 105, 1459–1469, 2000.

LIN, J.C., D. Brunner, and G. Gerbig.: Studying atmospheric transport through Lagrangian Models, Eos, Transactions, American Geophysical Union, Vol.92, No. 21, 177-184, 2001.

NEININGER, B., W. Fuchs, and M. Baeumle: A small aircraft for more than just ozone: Metair's' Dimona after ten years of evolving development, in: 11th Symposium on Meteorological Observations and Instrumentation, Amer. Met. Soc., Boston, 123–128, 2001.

NEININGER, B.: General description of data formats and parameters for all campaigns in 2008/ 2009, manuscript, 2009.

NEININGER, B.: First airborne in-situ measurements of Eyjafjallajökull's plume over Centrale Europe by METAIR-DIMO, draft manuscript for ACAM Barcelona, 2010.

PRATA, A. J. and A. Tupper: Aviation hazards from volcanoes: the state of the science, Nat. Hazards, 51, 239–244, 2009.

PETERSEN, G. N.: A short meteorological overview of the Eyjafjallajökull eruption 14 April-23 May 2010, Weather, 65, 203-207, 2010.

SCHUMANN, U., B. Weinzierl, O. Reitebuch, H. Schlager, A. Minikin, C. Forster, R. Baumann, T. Sailer, K. Graf, H. Mannstein, C. Voigt, S. Rahm, R. Simmet, M. Scheibe, M.

Lichtenstern, P. Stock, H. Rüba, D. Schäuble, A. Tafferner, M. Rautenhaus, T. Gerz, H. Ziereis, M. Krautstrunk, C. Mallaun, J.-F. Gayet, K. Lieke, K. Kandler, M. Ebert, S. Weinbruch, A. Stohl, J. Gasteiger, H. Olafsson, and K. Sturm: Airborne observations of the Eyjafjalla volcano ash cloud over Europe during air space closure in April and May 2010, Atmos. Chem. Phys. Discuss., 10, 22131–22218, 2010.

SCHUMANN, U., R.Baumann, A. Minikin, O. Reitebuch, T. Sailer, H. Schlager, C. Voigt, and B.Weinzierl: The volcanic ash plume near the Eyjafjallajökull in April/May 2010, Geophysical Research Abstract, Vol. 13, 2011.

SMITHONIAN INSTITUTION: Large explosions from the summit crater; ash plumes close airspace in Europe, Bulletin of the Global Volcanism Network, Bulletin 03/04/05, 2010.

STOHL, A., C. Forster, A. Frank, P. Seibert, G. and Wotawa: Technical note: The Lagrangian particle dispersion model FLEXPART version 6.2., Atmos. Chem. Phys., 5, 2461–2474, 2005.

STOHL A., A. J. Prata, S. Eckhardt, L. Clarisse, A. Durant, S. Henne, N. I. Kristiansen, A. Minikin, U. Schumann, P. Seibert, K. Stebel, H. E. Thomas, T. Thorsteinsson, K. Torseth, and B. Weinzierl: Determination of time- and height-resolved volcanic ash emissions and their use for quantitative ash dispersion modeling: the 2010 Eyjafjallajokull eruption, Atmos. Chem. Phys., 11, 2011.

STURKELL, E., P. Einarsson, F. Sigmundsson, A. Hooper, Space Systems, H. Geirsson, and H. Olafsson: Katla and Eyjafjallajökull Volcanoes, Sciences New York, 13, 5-21, 2010.

THOMAS, H. E., and A.J. Prata: Sulphur dioxide as a volcanic ash proxy during the April–May 2010 eruption of Eyjafjallajökull Volcano, Iceland, Atmos. Chem. Phys. Discuss., 11, 7757-7780, 2011.

TSI: Scanning Mobility Particle Sizer Spectrometer 3034, URL: http://www.tsi.com/en-1033/models/3286/3034.aspx, Access: 4. May 2011, 2011.

USGS (US GEOLOGICAL SURVEY): Volcano Hazards Program; Volcanic gases and their effects, URL:http://volcanoes.usgs.gov/hazards/gas/index.php, Access 5. June 2011, 2011.

WALL, R., and J. Flottau: Out of the ashes: Rising losses and recriminations rile Europe's air transport sector: Aviation Week & Space Technology, 172, 16, 23-25, 2010.

WHITE, J.D.L.: Impure coolants and interaction dynamics of phreatomagmatic eruptions, Journal of Volcanology and Geothermal Research, 74, 3-4, 155-170, 1996.

Acknowledgements

I would like to show my gratitude to my supervisor Stefan Brönnimann who was willing to guide me through my work, refining the master thesis and being a very interesting dialogue partner.

Also, I would like to thank my advisors Bruno Neininger providing Metair data and making it possible to combine my two favourites meteorology and aviation; as well as Ralph Rickli for the educational time and the pleasurable versatile conversations at Meteotest and his elusive expertise regarding meteorology.

My friends and family encouraged me on every occasion and thereby helped me trough the lows between the highs. Thanks to their backing, this half-year-fabric became much more aerodynamic!

Lastly, I offer my regards to all those who supported me in any respect during the completion of my master thesis.

Sandra Meisser

Declaration

under Art. 28 Para. 2 RSL 05

Last, first name: Meisser Sandra

Matriculation number: s 05-719-083

Programme: M.Sc. in Climate studies, Oeschger Centre, University of Bern

Bachelor ☐ Master X Dissertation ☐

Thesis title: Particle and trace gas measurements of Eyjafjallajökull 2010

Evolution and ageing of the volcanic ash cloud within Switzerland

Thesis supervisor: Dr. Stefan Brönnimann

I hereby declare that this submission is my own work and that, to the best of my knowledge and belief, it contains no material previously published or written by another person, except where due acknowledgement has been made in the text. In accordance with academic rules and ethical conduct, I have fully cited and referenced all material and results that are not original to this work. I am well aware of the fact that, on the basis of Article 36 Paragraph 1 Letter o of the University Law of 5 September 1996, the Senate is entitled to deny the title awarded on the basis of this work if proven otherwise.

Cham, 1.11.2011

Place, date

Signature